

Evolution of submarine canyons and hangingwall fans systems in fault-controlled margins: insights from geomorphic experiments and morphodynamic models: Insights from physical experiments

5 Steven Y. J. Lai¹, David Amblas², Aaron Micallef³, ~~Thomas P. Gerber⁴~~, and Hécervé Capart⁵Capart⁴:

¹Department of Hydraulic and Ocean Engineering, National Cheng Kung University, Tainan, Taiwan

²GRC Geociències Marines, Dept. de Dinàmica de la Terra i de l'Oceà, Universitat de Barcelona, Barcelona, Spain

³Marine Geology and Seafloor Surveying, Dept. of Geosciences, University of Malta, Msida, Malta ~~onerey Bay Aquarium Research Institute, Moss Landing, USA~~

10 ⁴Equinor—Research and Technology, Austin, Texas, USA

⁵~~Department~~⁴Department of Civil Engineering, National Taiwan University, Taipei, Taiwan

Correspondence to: Steven Y. J. Lai (stevenyjlai@mail.ncku.edu.tw)

Abstract. Tectonics play a significant role in shaping the morphology of submarine canyons, which form essential links in source-to-sink (S2S) systems. It is difficult, however, to investigate the resulting morphodynamics over long term. For this purpose, we propose a novel experimental approach that can generate submarine canyons and hangingwall fans on continuously evolving active faults. We utilize morphometric analysis and morphodynamic models to understand the response of these systems to fault slip rate (V_f) and inflow discharge (Q). Our research reveals several key findings. Firstly, the fault slip rate controls the merging speed of submarine canyons and hangingwall fans, which in turn affects their quantity and spacing. Additionally, the long profile shapes of submarine canyons and hangingwall fans can be decoupled into a gravity-dominated breaching process and an underflow-dominated diffusion process, which can be described using a constant-slope relationship and a morphodynamic diffusion model, respectively. Furthermore, both experimental and simulated submarine canyon-hangingwall fan long profiles exhibit strong self-similarity, indicating that the long profiles are scale independent. The Hack's scaling relationship established through morphometric analyses serves as an important link between different scales in S2S systems, bridging laboratory-scale data to field-scale data and submarine to terrestrial relationships. Lastly, for deep-water sedimentary systems, we propose an empirical formula to estimate fan volume using canyon length, and the comparison results from 26 S2S systems worldwide show a strong agreement. Our geomorphic experiments provide a novel perspective to understand deep-water sedimentary processes influenced by tectonics. The scaling relationships and empirical formulas we have established aim to assist in estimating volume information that is difficult to obtain during long-term landscape evolution processes. Different fault settings make the morphology of submarine canyon-fan systems on active margins complex and diverse. In this study we explore the continuum of erosion, transport and sedimentation processes taking place in fault-

格式化: 英文 (英國)

格式化: 字型: Times New Roman

格式化: 左右對齊

格式化: 字型: Times New Roman

格式化: 英文 (英國)

格式化: 字型: Times New Roman, 英文 (英國)

格式化: 英文 (英國)

格式化: 字型: Times New Roman

格式化: 字型: Times New Roman, 英文 (英國)

格式化: 英文 (英國)

格式化: 字型: Times New Roman, 英文 (英國)

格式化: 英文 (英國)

格式化: 字型: Times New Roman, 英文 (英國)

格式化: 英文 (英國)

格式化: 字型: Times New Roman, 英文 (英國)

格式化: 英文 (英國)

格式化: 字型: Times New Roman

controlled canyon-fan systems by using physical experiments and a morphodynamic model. Based on morphometric analyses we show how Hack's scaling relationships exist in submarine canyons and fans. The DEM of differences (DoDs) demonstrate the growth patterns and allow to establish relevant relationships between volumes of canyons and their corresponding fans. We reveal strong self-similarities on canyon-fan long profiles and, through a new morphodynamic model, we capture their evolution over time, including the trajectory of internal moving boundaries. We observe that fault slip rate controls the merging speed of coalescent submarine canyon-fan systems and, when coupling fault slip rate with inflow discharge, a competitive influence arises. In this study we also uncover scaling relationships spanned from laboratory to field-scale. Overall, our findings are inspiring and valuable for field investigators and modelers to better interpret and predict the morphological evolution and sedimentary processes of submarine canyon-fan systems in active fault settings.

格式化: 英文(英國)

Short summary (500-character plain text)

This study explores the creation of submarine canyons and hangingwall fans on active faults. It emphasizes the role of fault slip rate in their merging speed and quantity, which can be defined by gravity-dominated breaching and underflow-dominated diffusion processes. The study also reveals the self-similarity in canyon-fan long profiles, uncovers the Hack's scaling relationship and proposes a formula to estimate fan volume using canyon length. This is validated by global source-to-sink systems, providing insights into deep-water sedimentary processes.

1 Introduction

Global bathymetric data have been widely used to provide an overview of the distribution and geological significance of submarine canyons on active and passive margins (Harris and Whiteway, 2011; Harris et al., 2014). Source-to-sink (S2S) systems describe the response of the Earth's surface to tectonic and climatic signals over geological times, from terrestrial drainages (source) to deep-sea fans (sink) (Sømme et al., 2009; Nyberg et al., 2018). Valuable scaling relationships between morphometric parameters and morphology have been established in the analyses of the S2S systems (Sømme et al., 2009; Nyberg et al., 2018; Bernhardt and Schwanghart, 2021; Soutter et al., 2021b; Bührig et al., 2022a; Bührig et al., 2022b). Recent modern data of S2S also highlight the significant influence of tectonics settings on canyon geomorphology (Soutter et al., 2021b; Bührig et al., 2022a; Bührig et al., 2022b). The constructed scaling relationships provide insights into sedimentary controls and basin evolution, and can even be used to predict relationships in systems lacking data (Sømme et al., 2009; Nyberg et al., 2018). The efficiency of sediment routing from land to the ocean depends on the position of submarine canyon heads with regards to terrestrial sediment sources. Bernhardt and Schwanghart (2021) finds that steep and narrow shelves, as well as resistant bedrock and high river-water discharge, facilitate shore-connected canyon occurrence. A recent study based on modern global bathymetric data identified potential predictors of canyon geomorphology and suggested that the relative magnitudes of canyon-margin erosion and intra-canyon deposition are similar across different settings (Bührig et al., 2022a). A similar metastudy examined the influence of tectonic settings on canyon geomorphology, revealing a consistent canyon

格式化: 定位停駐點: 不在 25.52 字元 + 46.78 字元

格式化: 字型: Times New Roman

格式化: 字型: 非粗體

格式化: 字型: 非粗體

格式化: 字型: 非粗體

65 geomorphology across various tectonic scenarios (Bührig et al., 2022b). Nevertheless, the study suggested that slope failure
might be more significant in passive-margin canyons compared to active ones. These findings enhance our understanding of
slope systems and the role of tectonic setting in shaping deep-water sedimentary systems. Submarine canyons and fans are
main physiographic elements in the deeper reaches of the source-to-sink continuum of sedimentary processes. While submarine
canyons are drainage features facilitating the transport of sediment from land and shelf to the deep sea, submarine fans
represent its final depositional destination in many cases. These sediments are mainly transported by different forms of gravity
70 flows, including turbidity currents, hyperpycnal flows and dense shelf water cascades (Mulder et al., 1995; Dadson et al., 2005;
Canals et al., 2006; Milliman and Kao, 2005; Piper and Normark, 2009; Puig et al., 2014; Talling et al., 2015; Ambias and
Dowdeswell, 2018 and referenees therein). Most of our knowledge about the evolution of submarine canyons and fans come
from field survey and interpretations on passive margins, but in fact, the number of submarine canyons on active margins is
higher than that on passive margins (Harris and Whiteway, 2011) and the occurrence of downslope gravity currents is even
75 more frequent (Dadson et al., 2005; Milliman and Kao, 2005).

Haida Gwaii, in the northern Pacific coast of Canada, provides good field examples that illustrate the evolution of canyon fan
80 systems in an active margin (Fig. 1a). Within just 37 km of the Haida Gwaii margin there are 48 submarine canyons showing
different degree of morphological influence by the Queen Charlotte Fault Zone (Harris et al., 2014). This large strike-slip fault
truncates most of the canyon toes and creates numerous slope-confined and hanging canyons, and a series of coalescing fans
(bajada)(Harris et al., 2014). Other similar examples can be found in offshore eastern Taiwan (Hsieh et al., 2020), offshore
northern Sicily (Lo Iacono et al., 2014; Gamberi et al., 2015), New Zealand (Mountjoy et al., 2009; Micallef et al., 2014a) and
along Makran active margin (Bourget et al., 2011).

85 In the past, morphometric analyses for fluvial drainage basins have been used to analyze submarine canyons and fans, and to
establish subaqueous sealing relationships and geomorphic process laws. Morphometric analyses can link morphological and
sedimentological relationships in the sediment routing system. The classic and widely used river classification (Horton, 1945;
Strahler, 1957) and the sealing relationship between river length and catchment area (Haek, 1957) have been widely applied
to seale submarine canyon length and its drainage area (Mitchell, 2005; Straub et al., 2007; Tubau et al., 2013; Micallef et al.,
90 2014b). Longitudinal profile analyses were also widely used in submarine canyons to establish general geomorphic process
laws (Mitchell, 2005; Gerber et al., 2009; Covault et al., 2011; Ambias et al., 2011, 2012; Brothers et al., 2013). In addition,
morphometric analyses were also applied to submarine fan classification to establish sealing relationships between channels
and lobes (Pettinga et al., 2018).

95 Other studies have explored the role of tectonics in shaping canyon morphology. For example, Covault et al. (2011)
differentiated submarine canyon longitudinal profiles based on their convexity or concavity, revealing distinct depositional
architectures corresponding to different continental-margin types. This study demonstrated that the shape of these profiles

格式化: 定位停駐點: 不在 25.52 字元 + 46.78 字元

格式化: 字型: Times New Roman

格式化: 字型: 非粗體

格式化: 字型: 非粗體

100 reflects the interplay between uplift, depositional relief construction, and erosion related to mass wasting, providing a basis for classifying deep-sea sedimentary systems. Soutter et al. (2021b) re-examined the factors influencing the concavity of submarine canyons by analyzing the long profiles of 377 canyons. Their results indicated that tectonics is the primary control on canyon concavity, with active margins hosting the least concave profiles. Bourget et al. (2011) found that the Makran accretionary prism, between Pakistan and Iran, exhibits variability in tectonics and fluvial input distribution, which affects the turbidite system architecture and sediment distribution. Hence, concluding the significance of Makran turbidite system as a contemporary model for deep-water sedimentary systems in convergent margin settings. Deep-water sedimentation on active margins involves complex sediment transport pathways, as highlighted by McArthur et al. (2022) in the Hikurangi subduction margin, where sediment input points and tortuous sediment dispersal corridors result in convoluted depositional systems, challenging simple models of basin fill.

格式化: 英文 (美國)

110 Concerning the distal part of S2S systems, recent studies on submarine fans have developed scaling relationships to estimate fan volumes, while the submarine hangingwall fans formed in syn-rift successions have distinct characteristics compared to traditional submarine fans. For instance, the study by Prélat et al. (2010) compared submarine lobes from six systems and identified two distinct populations related to basin floor topography. Despite differences in configurations and sediment supply, these lobes share similar characteristics. The study also concludes that basin floor topography influences lobe geometry, while channel avulsion influence lobe volumes. In a recent study, morphometric analysis of submarine fans revealed scaling relationships between channels and lobe-shaped bodies, providing insight into their architectural development (Pettinga et al., 2018). The study demonstrated that scaling relationships exist between channel dimensions and lobe-shaped body dimensions, allowing for the prediction of lobe body volume and depositional area. Unlike traditional submarine fans, submarine hangingwall fans were identified in syn-rift successions. For instance, McArthur et al. (2013) investigated the stratigraphic development of an Upper Jurassic syn-rift succession in the Inner Moray Firth Basin, in northeastern Scotland. The study showed that sedimentation rates varied throughout different phases of rifting, with overall rates comparable to other deep marine rift basins. Barrett et al. (2021) also demonstrated that the volume of footwall-sourced hangingwall fans (Leeder and Gawthorpe, 1987) can be compared to the volume of material eroded from the fault scarp, revealing areas of sediment bypass and areas fed by sediment sources beyond the degraded fault scarp.

格式化: 字型: 非粗體

格式化: 字型: 非粗體

格式化: 字型: 非粗體

125 Compared to S2S studies and field surveys, only a few investigations have used numerical models or geomorphic experiments to study the long-term evolution of submarine canyons and fans. For example, a numerical surface process model was presented to examine submarine erosion processes caused by landslides and hyperpycnal flows (Petit et al., 2015). Their model demonstrated that the frequency of hyperpycnal flows largely influences the development of submarine canyons, and that an increase in the submarine slope accelerated erosion and the formation of a more dendritic canyon network. Additionally, a hydraulic-based stratigraphic forward model was used to investigate the impacts of morphological parameters on sediment budget partitioning and the channel network of delta-canyon-fan systems on passive margins (Wan et al., 2021; Wan et al.,

格式化: 字型: 非粗體

2022). Their model demonstrated that submarine canyons retreat landward, tributaries develop on the outer banks of canyons, and blind canyons expand landward. They concluded that the upslope pattern remains dominant regardless of changes in fluvial discharge and morphologies.

In terms of geomorphic experiments, pioneer micro-scale tank experiments were conducted to investigate the incision of a sediment bed by a gravity current (Métivier et al., 2005; Weill et al., 2014). The results indicated that the slope influences the erosion rate and channel incision speed, while brine discharge controls the channel geometry. Lai et al. (2016) emphasized the influence of tectonics on submarine canyon morphology and demonstrated that by isolating two key processes – the progressive growth of slope relief and a constant source of unconfined gravity flows – it is possible to produce a canyon growth sequence and morphologies that resemble those observed in the field. The study showed that unconfined gravity flows create featureless submarine slopes, whereas flows cascading across the shelf break result in deeply incised canyons with well-developed channel networks. Geomorphic experiments on self-channelized subaqueous fans revealed the formation, migration, and abandonment of well-defined depocenters characterized by channels bounded levees (Cantelli et al., 2011). The overall pattern of grain-size variation is downstream fining, with sediment in the channels being coarser than in the levees. Similar experiments further demonstrated the crucial role of the break in slope in channel aggradation and lobe architecture (Fernandez et al., 2014). Geomorphic experiments were also conducted to study submarine fans formed by sediment-laden flows. Ferguson et al. (2020) found that depositional relief and compensational stacking led to markedly different deposits during waxing and waning phases. Soutter et al. (2021a) demonstrated that different types of topographic confinement affect turbidites and erosion, leading to variations in deposit thickness, bifurcation, onlap, lateral spreading, and plunge-pool formation.

Among these geomorphic experiments, very few studies have examined the long-term evolution of submarine canyons and fans under the joint of tectonics and gravity flows. To pursue this avenue, the present study improves the experimental method of Lai et al. (2016) and proposed a novel experimental approach to examine the ongoing development of submarine canyons and hangingwall fans with density underflows on a continuously descending active fault. Through morphometric analysis and morphodynamic modelling, we aim to understand the response of submarine canyons and hangingwall fans to fault slip rate (V_f) and inflow discharge (Q), and to establish cross-scale scaling relationships to facilitate the estimation of volumetric data during the evolutionary process, a challenging task in field studies. The objectives of this study include: (1) establishing high-resolution digital elevation models (DEMs) through physical experiments; (2) developing laboratory-scale morphometric analysis and establishing scaling relationships between parameters; (3) comparing long profiles of canyons and hangingwall fans between experiments and morphodynamic models; (4) identifying self-similarity within the system; (5) proposing scaling relationships and empirical formulas across scales, extending from laboratory setup to the natural environment.

However, the time scale for forming a submarine canyon fan system is much longer than a human timescale, making direct measurements of the evolving processes rarely possible. These difficulties have led researchers to turn to experimental studies of submarine canyons and fans. Past physical experiments confirmed that the subaqueous erosional channelized morphology

格式化: 字型: 非粗體

170 produced by long-lived gravity currents can be reproduced using saline underflow and plastic sediment (Metivier et al., 2005). Subsequent experimental studies also pointed out that slope controls the rate of erosion and the speed of channel incision, while saline discharge affects the width and depth of submarine canyons (Weill et al., 2014). In different approaches, Lai et al. (2016) demonstrated that laboratory experiments can generate autogenic, deeply incised submarine canyons with well-developed drainage features by using salt water acting on silica paste with submerged stepwise lowering base level. These authors also revealed that the submarine canyon long profile in evolution are time and scale independent. Apart from the canyon experiments, laboratory turbidity currents can generate self-channelized submarine fans with leveed channels that gradually shift and avulse (Yu et al., 2006). Further experiments showed that repeated turbidity currents can also produce levee-bounded submarine channels and stacked lobes (Cantelli et al., 2011), and that the break in slope controls channel aggradation and lobe architecture (Fernandez et al., 2014).

180 The purpose of this study is to explore the erosion-transport-sedimentation processes involved in the evolution of submarine canyon-fan systems in fault-controlled margins. For this we use physical experiments and a morphodynamic model that allow to define general geomorphic laws. The aims of this study are: (1) to obtain high-resolution digital elevation models (DEMs) for the canyon-fan evolutionary surfaces; (2) to develop laboratory-scale morphometric analyses and to establish scaling relationships between parameters; (3) to investigate scale-independent self-similarities in long profiles; (4) to propose a morphodynamic model that allow to predict fan volumes based on canyon lengths.

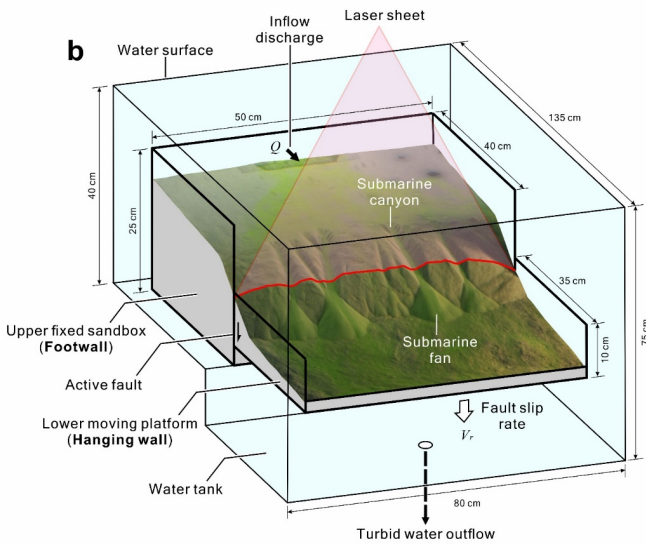
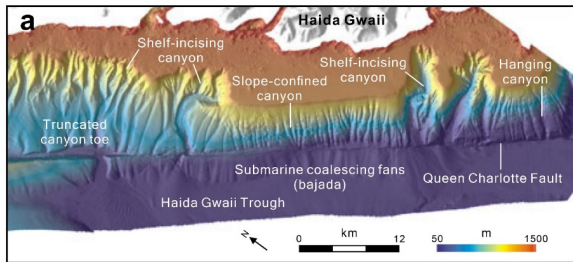


Figure 1. (a) Seafloor morphology offshore Haida Gwaii (modified from Barrie et al., 2013 and Harris et al., 2014); (b) Experimental setup for studying the evolution of submarine canyon-fan systems in an active fault setting.

2 Methods

2.1 Experimental design

To simulate a basic submarine fault setting that mimics the morphology observed offshore Haida Gwaii, a novel experimental set-up, containing a water tank (135 cm long, 80 cm wide and 75 cm deep) and a submerged sedimentary basin (75 cm long,

格式化: 左右對齊

已註解 [賴悅仁1]: 圖中的標註要修改, 要用 hangingwall fans. "hangingwall"

格式化: 字型: Times New Roman

格式化: 內文, 定位停駐點: 25.52 字元, 中 + 46.78 字元, 右

格式化: 字型: Times New Roman

190 ~~50 cm wide and 25 cm deep), tank (135 cm long, 80 cm wide and 75 cm deep)~~ was designed to ~~recreate~~ investigate the evolution of a submarine ~~canyons and hangingwall fans, fault with 90-degree dip angle~~ (Fig. 1b). This submerged tank ~~sedimentary basin~~ consists of an upper fixed sandbox (as a footwall) and a lower moving platform (as a hanging-wall). The hanging-wall was controlled by a motor with adjustable speed to simulate different fault slip rate (V_r) ~~of 90-degree dip angle~~. Very fine silica sand ($d_{50} = 0.1$ mm) and kaolinite (proportion 100:1 by weight, as suggested by Hasbargen and Paola, 2000 and Lai et al., 2016) were well mixed and filled into the submerged sandbox and platform as an erodible substrate. Upstream, different inflows discharge (Q) of saturated brine (density $\rho_{in} = 1200$ kg/m³) were used as unconfined downslope ~~high-density, gravity turbidity currents for modeling long lived hyperpycnal flows or mud rich turbidity currents for transporting sediment along submarine canyons and hangingwall fans~~ (Métivier et al., 2005; Spinewine et al., 2009; Sequeiros et al., 2010; Weill et al., 2014; Foreman et al., 2015; Lai et al., 2016; 2017). This approach contrasts to other experiments ~~using dilute turbidity currents for forming classical submarine fans~~ (Cantelli et al., 2011; Fernandez et al., 2014; Ferguson et al., 2020; Soutter et al., 2021a).

格式化: 字型: Times New Roman

215 ~~Run A1, Run B1 and Run C1) and \approx 5 min for the runs with relatively faster fault slip rate (i.e., Run A2, Run B2 and Run~~
~~C2), depending on the fault slip rate.~~ Time-lapse photography was used to record the evolution of submarine canyon-fan
 systems every 5 s for each experiment. Without draining out the ambient water, the inflow was turned off to form a temporarily
 frozen landscape at ~~the end of~~ each stage ~~end~~. ~~Then the~~ newly generated submarine landscape was ~~then~~ scanned. A
 topographic imaging system (Lai et al., 2016; Lai et al., 2017; Huang et al., 2023) was used to construct high-resolution (1
 220 mm ~~\times~~ 1 mm) digital elevation models (DEMs), orthorectified images and gradient maps over successive stages.

格式化: 字型: Times New Roman

格式化: 字型: (中文) 新細明體, (中文) 中文 (台灣)

Table 1. Summary of experimental conditions.

Run	Inflow discharge Q (mm^3/s)	Fault slip rate V_f (mm s^{-1})	Stage interval (min)	Total stages
A1	1600	0.025	10	9
A2	1600	0.049	5	9
B1	3300	0.026	10	9 8
B2	3500	0.041	5	11 9
C1	5000	0.014	10	12 12
C2	800	0.064	5	7

格式化表格

格式化: 上標

225 2.2 Morphometric definitions of submarine canyons and hangingwall fans

~~Landscape features~~ Morphological features of submarine canyons and hangingwall fans systems were defined prior to applying
 the morphometric analyses-analysis (Fig. 2a). First, the fan apex was defined at the most upstream point of a submarine fan,
 or the intersection between two fan edge asymptotes. Then, canyon length (L_c) was defined as the maximum path from the
 canyon head to its fan apex; canyon width (W_c) was defined as the width of the ~~canyon~~-bounding box for a canyon; canyon
 230 area (A_c) was the area of a canyon drainage. Similarly, fan length (L_f) was the maximum path from the fan apex to its fan toe;
 fan width (W_f) was the width of the fan-bounding box for a fan; fan area (A_f) was the area of a fan deposit.

格式化: 字型: (英文) Times New Roman

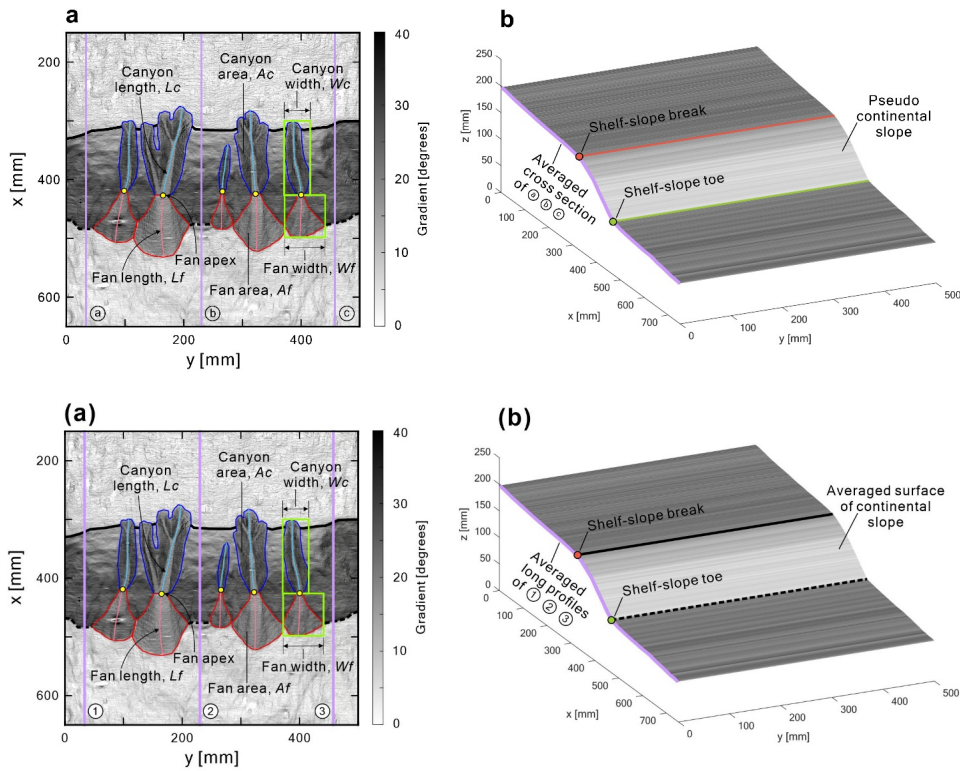
The volumes of submarine canyons and hangingwall fans can be obtained by subtracting the pseudo continental slope from
 the DEM of each stage (Fig. 2b). First, three ~~cross-sections~~ long profiles were extracted from the DEM, which were unaffected
 235 by saline underflows (e.g., ~~cross-sections~~ long profiles a1, b-2 and e-3 in Fig. 2a). The averaged ~~cross-section~~ long profiles
 were then used to create an ~~pseudo-averaged surface of~~ continental slope for that stage (Fig. 2b). Next, the ~~pseudo-averaged~~
~~surface of~~ continental slope was subtracted from the DEM to obtain the DEM of difference (DoD). Negative values represent
 canyon incision depths; positive values ~~show~~ represent fan thicknesses. In addition, the ~~(x, z)~~ coordinates of the shelf slope

格式化: 字型: Times New Roman

格式化: 字型: Times New Roman

break and shelf slope toe were recorded from the pseudo-continental slope to understand the evolution of these two internal moving boundaries. The moving trajectories will be shown in Section 3.2.

240



245 **Figure 2. (a) Morphometric definitions of submarine canyons and hangingwall-fans systems. Yellow dots are fan apices of hangingwall fans. Green rectangles are bounding boxes. Thick black solid line is shelf-slope break; Thick black dash line is shelf-slope toe. (b) Reconstructed pseudo-averaged surface of continental slope unaffected by downslope gravity saline under-flows.**

250

格式化: 定位停駐點: 不在 25.52 字元 + 46.78 字元

格式化: 左右對齊

格式化: 字型: Times New Roman

2.3 Geometric and Morphodynamic models

The formation of a submarine canyons and hangingwall fans system involves simultaneous erosion on the footwall and deposition on the hangingwall (Fig. 3), which resembles the knickpoint smoothing process observed in submarine canyons (Mitchell, 2006) and fluvial process across an active faults (Hanks et al., 1984) and the knickpoint smoothing process observed in submarine canyons (Mitchell, 2006). Based on these geomorphic characteristics, with this similar concept, we decoupled the formation into two different processes: (1) an evolving continental slope (Fig. 3b), which can be model by a constant-slope geometric model driven by a normal fault (Fig. 3b); and (2) the evolution of a submarine canyon and hangingwall fan (Fig. 3c), which can be simulated by a simple morphodynamic model driven by an underflow system driven by a downslope gravity flow (Fig. 3c). a one-dimensional morphodynamic model was developed for describing a fault-controlled submarine canyon fan evolution, driven by downslope gravity flows (Fig. 3).

For the continental slope (Fig. 3b). First, the position of the active fault was set to $x = 0$. Then, the submarine canyon fan evolution was decoupled into two different processes: (1) an evolving continental slope driven by a normal fault (Fig. 3b); (2) a submarine canyon fan system driven by a downslope gravity flow (Fig. 3c). As the hanging wall continues to fall, the continental slope was is mainly formed by avalanching process, with its slope kept at the angle of repose ($S_s = 38^\circ$). The retreating shelf-slope break and advancing shelf-slope toe can be described by the following geometric relationships (Eq. (1) and Eq. (2)) (modified from Lai et al., 2016);

$$(x, z)_{ssb} = \left(\frac{-H_1}{S_s - S_1}, \frac{S_1 H_1}{S_s - S_1} \right) \quad (1)$$

$$(x, z)_{sst} = \left(\frac{H_2}{S_s - S_2}, \frac{-S_2 H_2}{S_s - S_2} \right) \quad (2)$$

where H_1 and H_2 are the upstream and downstream knickpoint heights; S_1 and S_2 are the upstream and downstream far field slopes, respectively. S_s is the inclination of continental slope.

For the submarine canyon and hangingwall fan (Fig. 3c), the entire long profile formed by downslope gravity flows can be described by a knickpoint smoothing diffusion process. Eq. (3) and (4) describes the entire submarine canyon fan long profile $z(x, t)$ of submarine canyon $z_1(x_1, t)$ and the long profile of hangingwall fan $z_2(x_2, t)$, respectively including both the footwall ($x_1 = x < 0$) and hanging wall ($x_2 = x > 0$):

$$z_1 z(x_1, t) = -H_1 H \cdot \operatorname{erf} \left(\frac{x_1^*}{2\sqrt{K_1 K t}} \right) - S_1 S x_1, \quad x_1 < 0 \quad (3)$$

$$z_2 z(x_2, t) = -H_2 \cdot \operatorname{erf} \left(\frac{x_2}{2\sqrt{K_2 t}} \right) - S_2 x_2, \quad x_2 > 0 \quad (4)$$

where H = knickpoint heights (shape factor); erf = error function (shape function); K = diffusivity; S = far-field slope. The first and second terms on the right-hand side of Eq. (3) and (4) account for the variations in bed profile caused by the geomorphic diffusion and initial bed slope, respectively. The Diffusion-diffusion processes on footwall and hanging-wall may

格式化: 字型: (中文) Times New Roman, 英文 (英國)

be different, suggesting that different parameters (H_1, K_1, S_1) and (H_2, K_2, S_2) can be used for the submarine canyons and hangingwall fans, upstream and downstream canyon-fan long profiles.

To investigate the self-similarity of the evolving canyon-fan long profiles in various settings, the first and second terms on the right-hand side of Eq. (3) and (4) were normalized, respectively, by the shape factor H_1 and H_2 , and the time-varying length scale $\sqrt{K_1 K t}$ and $\sqrt{K_2 t}$, respectively. Then the normalized profiles \bar{z}_1 and \bar{z}_2 is time-varying only as a function of the dimensionless horizontal coordinate $\sigma_1 \varphi (= x_1 \varphi / \sqrt{K_1 K t})$ and $\sigma_2 (= x_2 / \sqrt{K_2 t})$ (Capart et al., 2007; Lai and Wu, 2021):

$$\bar{z}_1(\sigma_1 \varphi) = -\text{erf}\left(\frac{\sigma_1 \varphi}{2}\right) - S_1 \sigma_1, \quad \sigma_1 < 0 \varphi \quad (45)$$

$$\bar{z}_2(\sigma_2) = -\text{erf}\left(\frac{\sigma_2}{2}\right) - S_2 \sigma_2, \quad \sigma_2 > 0 \quad (6)$$

The comparison between diffusion model and experiments will be presented in Section 3.2.

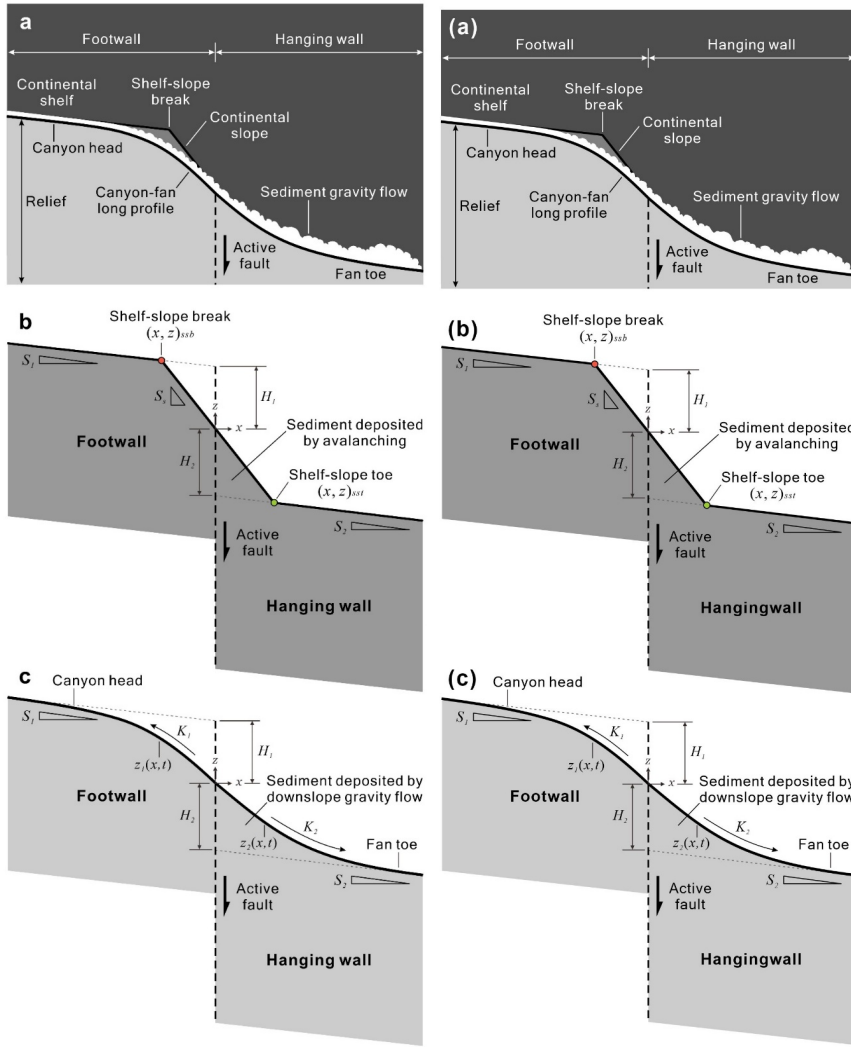


Figure 3. (a) The formation of submarine canyons and hangingwall fans Geomorphic components for a one-dimensional evolving submarine canyon-fan long system. (b) Mathematical geometric definitions for an the evolution

of evolving continental slope (modified from Lai et al., 2016) governed by gravity-induced avalanching process. (c) Mathematical morphodynamic definitions for the evolution of submarine canyons and hangingwall fans (modified from Lai and Wu, 2021) long profile driven by downslope gravity flows.

3 Results

3.1 Morphological Evolution evolution of submarine canyons and hangingwall fans systems

The geomorphic experiments documented the initiation and complex development of submarine canyons and hangingwall fans (Fig. 4). Taking Run B1 as an example, the fault location in the experiment was at $x = 400$ mm (Fig. 4a). Once the experiment began, the hangingwall steadily descended at a rate of $V_r = 0.026$ mm s^{-1} , while the upstream released saline water with a discharge of $Q = 3300$ mm³ s^{-1} . As the hangingwall continued to descend, the shelf-slope break retreated upstream and the shelf-slope toe extended downstream (Fig. 4c). Along the slope where the saline underflow passed, a series of submarine canyons and hangingwall fans formed. In areas without saline underflow, the slope maintained a fixed angle (approximately 38°, the angle of repose of the material). At $t = 30$ min (Fig. 4d), four distinct canyon-hangingwall fan systems (Systems A, B, C, and D) emerged on the continental slope. Additionally, slope-confined canyons occurred between Systems B and C (Fig. 4e), with their canyon heads located below the shelf-slope break. By $t = 70$ min (Fig. 4h), these four canyon-hangingwall fan systems continued to grow, but the original slope-confined canyons had nearly disappeared. At $t = 90$ min (Fig. 4j), System A vanished, while Systems B and C still maintained shelf-incising canyons. On the other hand, System D transformed into a slope-confined canyon. For detailed evolution processes of each run, please refer to Fig. S1 to Fig. S6 and Video S1 to Video S6 in the supplementary information. Physical experiments simulated the initiation and evolution of submarine canyon fan systems driven by downslope gravity flows in normal fault settings (Fig. 4). The fault line was at a fixed location ($x = 400$ mm) and as the hanging wall started to fall, the continental slope expanded simultaneously both upstream and downstream, but keeping its bed slope at the angle of repose (38°). At the same time, saline gravity flows formed submarine canyons and fans on the slope. When $t = 10$ min, tiny gullies and fans appeared at the base of the continental slope. At $t = 30$ min, small gullies merged into several shelf incising canyons and a few slope-confined canyons. When $t = 40$ min, shelf incising canyons developed their own tributaries. At $t = 50$ min, four major submarine canyon fan systems maintained on the continental slope. At $t = 70$ min, the four major systems continued to grow, but the slope-confined canyons completely disappeared. At $t = 80$ min, System C appeared obvious fan terraces. When $t = 90$ min, System A disappeared, and Systems B and C remained kept as mature shelf incising canyon fan systems; System D transformed into a slope-confined canyon fan system. See Fig. S1 to Fig. S6, Table S1 to Table S6 and Movie S1 to S6 for detailed evolution processes.

格式化: 字型: (英文)Times New Roman

格式化: 字型: 非粗體

格式化

格式化: 字型: Times New Roman

Hillshaded gradient maps demonstrated the details of submarine canyons and hangingwall fans, as well as the similarities and dissimilarities between different runs (Fig. 5). In Series A (Fig. 5a and Fig. 5b), the inflow discharge was constant ($Q = 1600 \text{ mm}^3 \text{ s}^{-1}$). The fault slip rate for Run A1 was $V_r = 0.025 \text{ mm s}^{-1}$, while the fault slip rate for Run A2 was $V_r = 0.049 \text{ mm s}^{-1}$. When Q was kept consistent, doubling the fault slip rate (Run A2, Fig. 5b) led to the rapid merge of canyons and hangingwall fans into a few major systems, with significant increases in the length, width, and area of the systems. In Series B (Fig. 5c and Fig. 5d), the inflow discharge ($Q \approx 3400 \text{ mm}^3 \text{ s}^{-1}$) was twice as large as in Series A, but the fault slip rate remained similar to Series A ($V_r = 0.026 \text{ mm s}^{-1}$ for Run B1, $V_r = 0.041 \text{ mm s}^{-1}$ for Run B2). Similarly, when the fault slip rate doubled (Run B2, Fig. 5d), canyons and hangingwall fans also rapidly merged into a few major systems, with significant increases in the length, width, and area of the systems. Lastly, Series C (Fig. 5e and Fig. 5f) presented two extreme cases. Run C1 demonstrated extremely high flow rate ($Q = 5000 \text{ mm}^3 \text{ s}^{-1}$) paired with an extremely low fault slip rate ($V_r = 0.014 \text{ mm s}^{-1}$), while Run C2 represented extremely low flow rate ($Q = 800 \text{ mm}^3 \text{ s}^{-1}$) paired with an extremely high fault slip rate ($V_r = 0.064 \text{ mm s}^{-1}$). Although the morphological differences in canyons and hangingwall fans produced under these extreme conditions were quite significant, the same conclusion held: V_r controlled the overall morphological evolution. For example, at $t = 70 \text{ min}$, Run C1 still had 7 canyon-hangingwall fan systems (Fig. 5e), whereas Run C2 maintained almost a single major system throughout the entire evolution process (Fig. 5f), with larger length, width, and area compared to all systems in Run C1. In summary, fault slip rate controlled the merging speed of submarine canyons and hangingwall fans, thereby influencing the quantity and spacing of the systems. The gradient maps calculated from each DEM demonstrated the morphological responses of submarine canyon-fan systems to the given parameters (Fig. 5). Under fixed inflow discharge, double the fault slip rate reduced the number of canyon-fan systems and made the systems become close-spaced (compare Fig. 5a to Fig. 5b and Fig. 5e to Fig. 5d). On the contrary, at fixed fault slip rate, double the inflow discharge resulted in similar size and number of submarine canyon-fan systems (compare Fig. 5a to Fig. 5c and Fig. 5b to Fig. 5d). When the fault slip rate and inflow discharge were extremely contrasted, the minimum fault slip rate formed a large number of slope-confined canyon-fan systems (Run C1, Fig. 5c). Conversely, the maximum fault slip rate resulted in a single shelf-incising canyon-fan system (Run C2, Fig. 5f) in early stages.

The DEM of differences (DoDs) showed the erosion and deposition patterns of canyons and fans for each stage (Fig. 6). When the inflow discharge was fixed, double the fault slip rate made the incision and deposition depths deeper and thicker, respectively (compare Fig. 6a to Fig. 6b and Fig. 6c to Fig. 6d). Conversely, when the fault slip rate was fixed, double the inflow discharge did not make significant differences to incision and deposition depths (compare Fig. 6a to Fig. 6c and Fig. 6b to Fig. 6d). When the fault slip rate and inflow discharge were extremely contrasted, the depths and volumes generated by the maximum fault slip rate (Run C2) were much larger than that of the minimum fault slip rate (Run C1) (Fig. 6e and Fig. 6f). Generally, the responses of DoDs to given parameters were similar to those responses observed in the gradient maps. The influence of fault slip rate and inflow discharge on the volumes of canyons and fans will be discussed in Section 4.

格式化: 字型: 非粗體

格式化: 字型: 非粗體

格式化: 上標

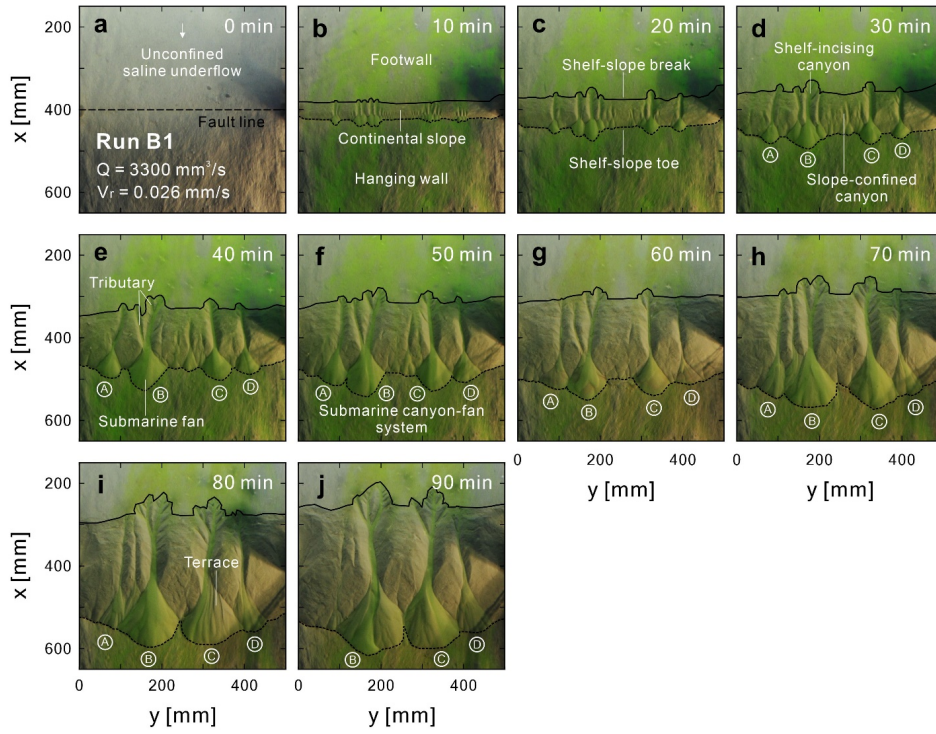
格式化: 非上標/下標

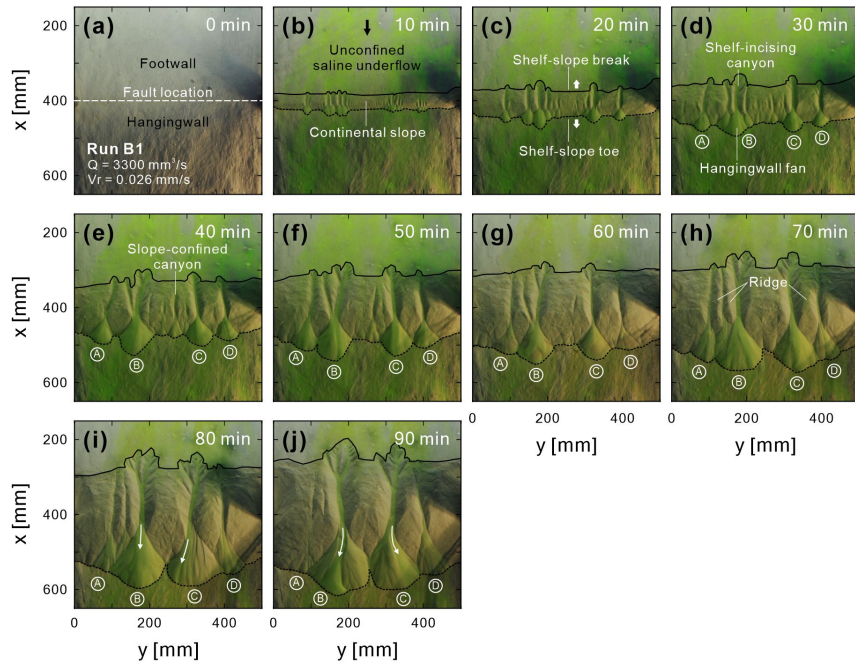
格式化: 上標

格式化: 上標

格式化: 字型: 非粗體

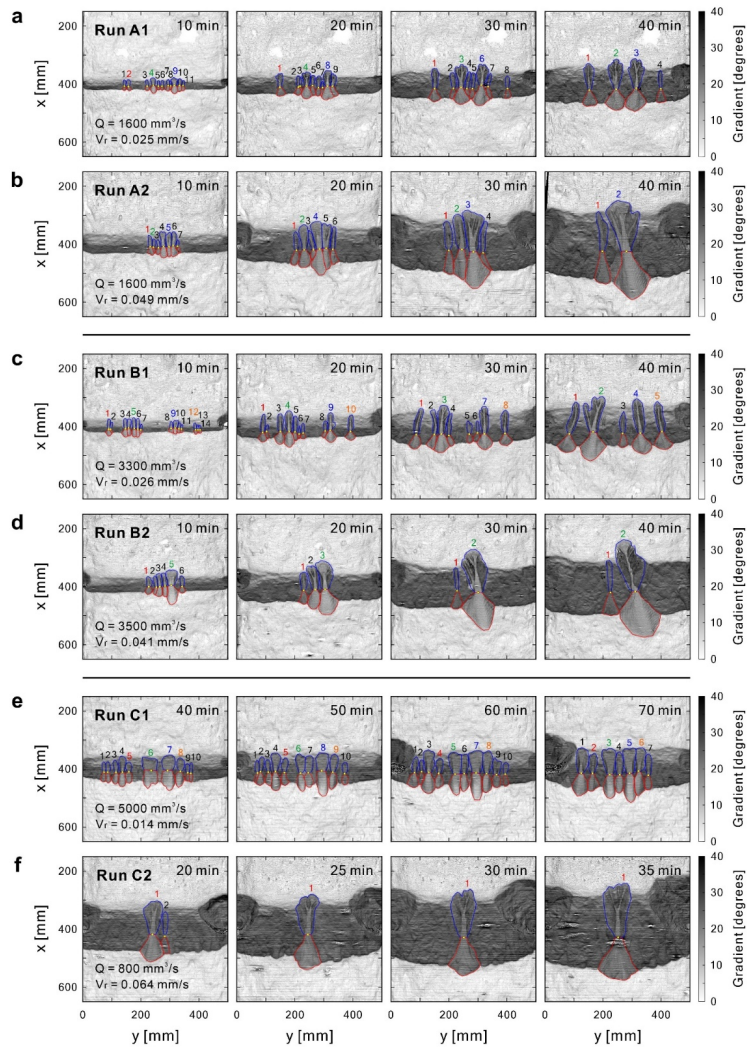
格式化: 字型: (中文) 新細明體, (中文) 中文 (台灣)





360

Figure 4. Observations from the orthophotos (Run B1 from $t = 0$ to 90 min). Systems A, B, C and D are the traced submarine canyon-fan systems across stages.



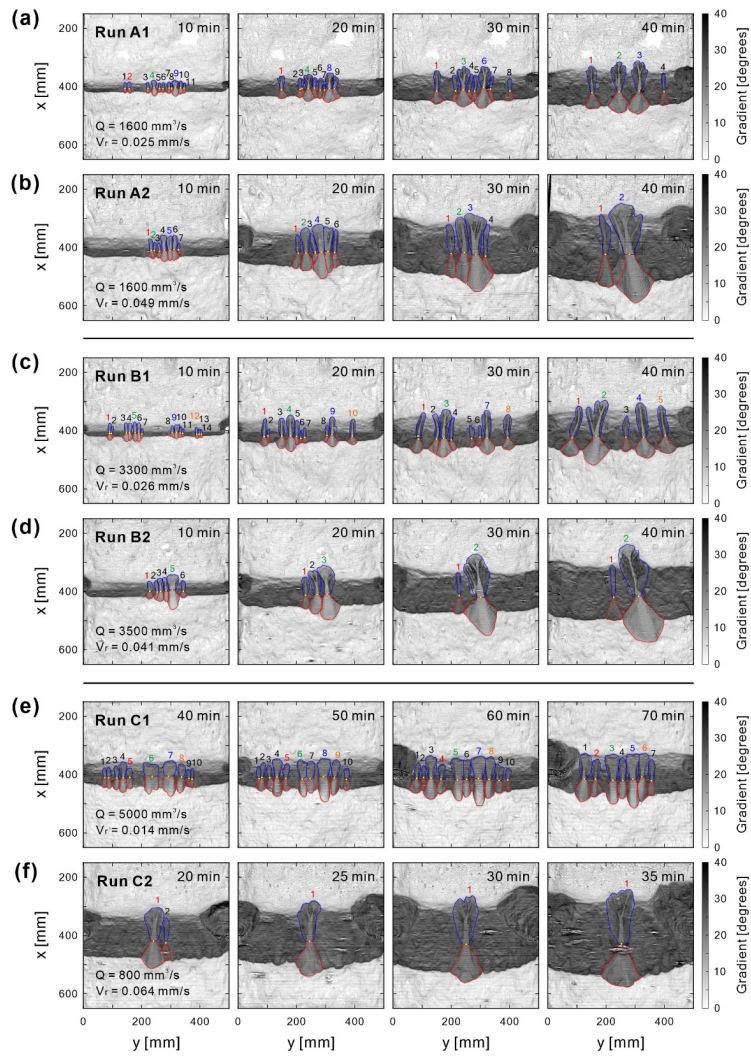
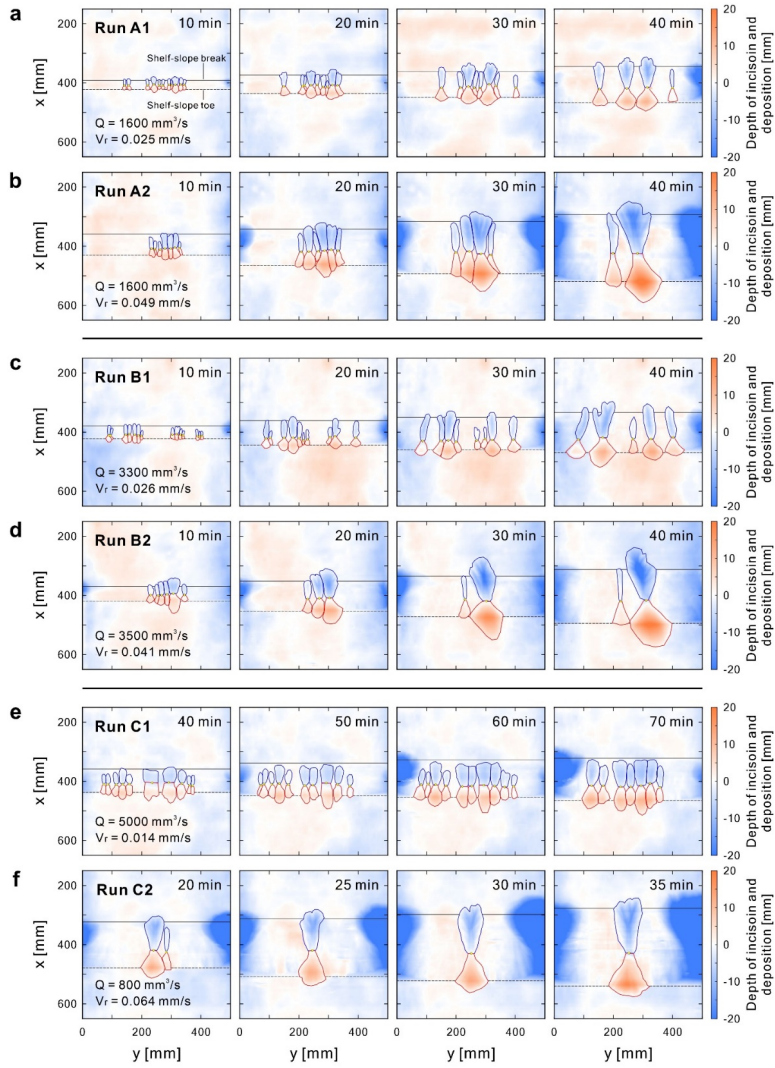


Figure 5. Hillshaded gradient maps for each run. Blue lines are the rims of submarine canyons. Red lines are the boundaries of submarine fans. Yellow dots are fan apices. Colored numbers represent the traced canyon-fan system

of each stage.



格式化: 左右對齊, 定位停駐點: 不在 25.52 字元 + 46.78 字元

Figure 6. DEM of differences (DoDs) for each run. The lines of shelf slope break and shelf slope toe were translated from the pseudo surface of each run.

3.2 DEM analysis of canyon erosion and fan deposition

375 The DEM of differences (DoDs) shows the erosion depth of submarine canyons and the deposition thickness of hangingwall fans (Fig. 6). For example, at $t = 30$ min, runs with lower fault slip rates, such as Run A1, Run B1, and Run C1 (Fig. 6a, Fig. 6b, and Fig. 6c, respectively), have shallower submarine canyon incision depths and hangingwall fan deposition thicknesses. In contrast, runs with higher fault slip rates, such as Run A2, Run B2, and Run C2 (Fig. 6d, Fig. 6e, and Fig. 6f, respectively), have deeper incision depths and deposition thicknesses. Additionally, since no sediment was added upstream in our experiments, the eroded sediment comes entirely from the substrate on the continental slope. The variations in the DoDs generated in the system are all related to changes in the bed load. Therefore, the volume of submarine canyons and their corresponding hangingwall fans are similar.

380

格式化: 字型: 非粗體

格式化: 字型: 非粗體

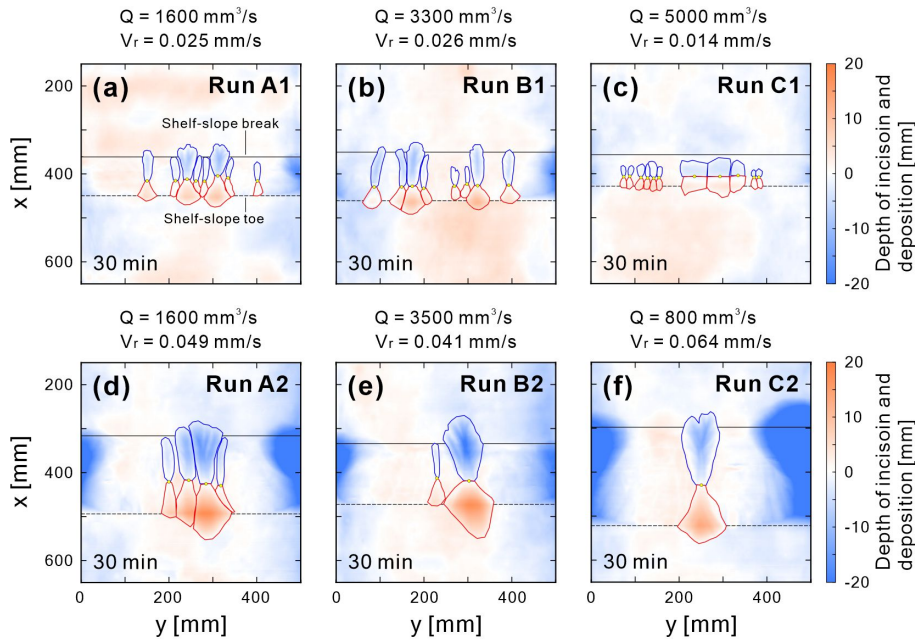
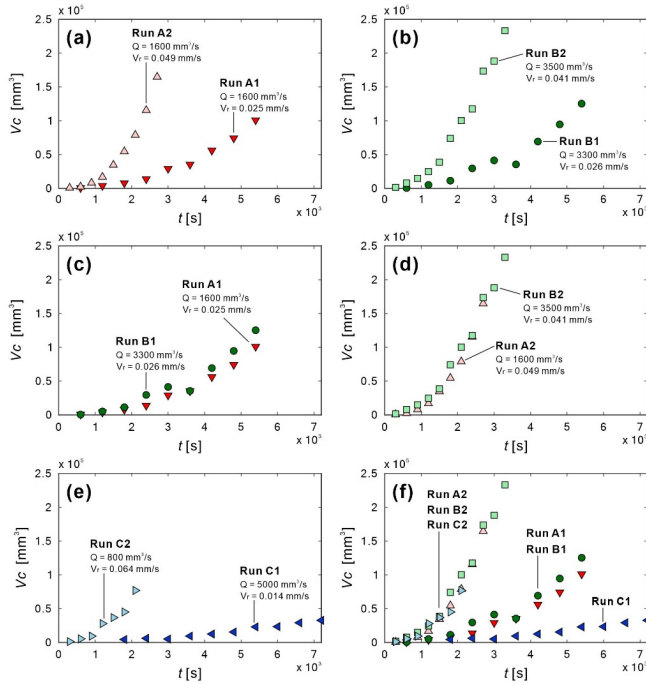


Figure 6. The DEM of differences (DoDs) for each run at $t = 30$ min.

385 The volume evolution of submarine canyon (V_c) demonstrates the influence of fault slip rate and inflow discharge on the system (Fig. 7). When the inflow discharge was fixed at $Q = 1600 \text{ mm}^3 \text{ s}^{-1}$, the fault slip rate of Run A2 was twice as large as Run A1 (Fig. 7a). At a fixed time, V_c of Run A2 was five times larger than Run A1. Similarly, when $Q = 3400 \text{ mm}^3 \text{ s}^{-1}$, the fault slip rate of Run B2 was twice as large as Run B1 (Fig. 7b), and the corresponding V_c followed the same trend. In contrast, when the fault slip rate was fixed at $V_f = 0.025 \text{ mm s}^{-1}$, although the inflow discharge of Run B1 was twice as large as Run A1 (Fig. 7c), there was little difference in V_c between Run B1 and Run A1 over time. Similarly, when the fault slip rate was fixed at $V_f = 0.045 \text{ mm s}^{-1}$ (Fig. 7d), the discharge of Run B2 was twice as large as Run A2, and the corresponding V_c was similar. This indicated that under fixed fault slip rate conditions, the magnitude of discharge did not cause significant variations in V_c . Finally, under extreme conditions, the slip rate of Run C2 was about five times larger than Run C1, although the flow rate of Run C2 was only $Q = 800 \text{ mm}^3 \text{ s}^{-1}$ (the smallest among all runs), the corresponding V_c of Run C2 was three times larger than Run C1.

390

395 All these results confirmed that fault slip rate had a more dominant influence on submarine canyons and hangingwall fans when compared to inflow discharge.



格式化: 字型: 非粗體

格式化: 置中

Figure 7. Time evolution for the eroded volume of submarine canyons (V_c).

3.2.3 Longitudinal profiles of Comparison of submarine canyons and hangingwall fans long profiles

The comparison between the experimental continental slopes and long profiles simulated by the geometric relationships (Eq. 1 and Eq. 2) is shown in Fig. 8. The continental slope was extracted from an area unaffected by saline underflow, representing the morphological result solely generated by gravity in the system. Although the continental slope at the laboratory scale rested at the angle of repose (approximately 38°), this was the ultimate result of mass wasting processes, including landslides, flow sliding, and gradual breaching. Despite the different fault slip rates given in different runs, the experimental continental slopes were consistent with the long profiles simulated by the geometric relationships. This indicates that the continental slope generated under different fault slip rates maintained a constant slope relationship at each stage. The comparison of experimental and simulated submarine canyon fan long profiles is shown in Fig. 7. The diffusion model captured the evolution of four major shelf-incising canyon-fan long profiles. The diffusion coefficients K_1 and K_2 controlled the long profile of canyon and fan, respectively. As the hanging wall continued to fall, the canyon fan long profile became smoother, indicating that the diffusion coefficients were not fixed values, but proportional to the knickpoint heights (H_1 and H_2). Contrary to the canyon fan long profiles, the continental slope was steep, straight and maintained at the angle of repose. The geometric relationship (Eq. (1) and Eq. (2)) well captured the evolution of continental slopes (Fig. 7c). Therefore, both the diffusion model and geometric relationships capture the essence of submarine canyon fan systems on an evolving continental slope.

The experimental long profiles of submarine canyons and hangingwall fans were compared to the morphodynamic model (Fig. 9). Using System A in each experiment as an example, the results show that the morphodynamic model captured the long-term evolution trends of submarine canyons and hangingwall fans. The diffusion coefficient K_1 in the model controls the development of the canyon thalweg, while the diffusion coefficient K_2 controls the development of the hangingwall fan. As the hangingwall continues to descend, the canyon-hangingwall fan long profile becomes smoother. This indicates that K_1 and K_2 are not fixed values but vary proportionally with the relief. Consequently, the morphodynamic model is validated and could be used to predict the long profile evolution of submarine canyons and hangingwall fans at laboratory scale.

Finally, both experimental and simulated submarine canyon-hangingwall fan long profiles plotted in dimensionless axes show strong self-similarity (Fig. 10). To investigate the self-similarity of the evolving long profiles during different stages of each run, the first and second terms on the right-hand side of Eq. (3) are, respectively, normalized by the shape factor H and the time-varying length scale \sqrt{Kt} . That is the upstream and downstream profiles, $\bar{z}_1(\sigma)$ and $\bar{z}_2(\sigma)$, are plotted against the dimensionless coordinates σ_1 and σ_2 . For each run, the scaled profiles of an evolving submarine canyon-hangingwall fan

格式化: 英文 (英國)

格式化: 字型: (英文)Times New Roman

格式化: 字型: 非粗體

430 collapse to a single diffusion-based theoretical profile (black solid line), indicating the establishment of morphological self-similarity consistently.

435 The trajectories of internal moving boundaries over time are shown in Fig. 8. The x -position of the four moving boundaries were shifted to the fault line ($x = 400$ mm) for distinguishing whether canyons and fans were in erosion or deposition relative to the continental slope. The results demonstrated that the trajectories of all internal moving boundaries over time were surprisingly linear. Systems B and C were deep shelf-incising canyons, for which their corresponding canyon incising distance (Δx_{in}) and fan advancing distance (Δx_{adv}) were longer. Conversely, Systems A and D were shallow shelf incising canyons, for which their corresponding Δx_{in} and Δx_{adv} were much shorter. See Fig. S12 to Fig. S16 for other moving trajectories.

440 On the dimensionless coordinates, both experimental and simulated long profiles showed strong self-similarities (Fig. 9). To investigate the self-similarity of the evolving profiles during different stages of each run, the first and second terms on the right hand side of Eq. (3) are, respectively, normalized by the shape factor H and the time-varying length scale \sqrt{Kt} . That is the upstream and downstream profiles, $\bar{z}_1(\sigma)$ and $\bar{z}_2(\sigma)$, are plotted against the dimensionless coordinates σ_1 and σ_2 . For instance, the four systems traced in Run B1 at different stages (35 long profiles in total) collapsed to a single curve and showed strong self-similarity (Fig. 9c). More surprisingly, the scaled submarine canyon fan long profiles of the other runs also collapsed to a similar theoretical profile, indicating that a morphological self-similarity was established consistently. In addition, the evolving continental slopes of each run also collapsed to the same geometric profile (red solid line). Therefore, these results confirmed that the submarine canyon fan long profiles and continental slopes evolved at different stages have strong, scale-independent self-similarities.

450

格式化: 字型: Times New Roman

格式化: 字型: Times New Roman

格式化: 字型: Times New Roman

格式化: 字型: Times New Roman, 非斜體

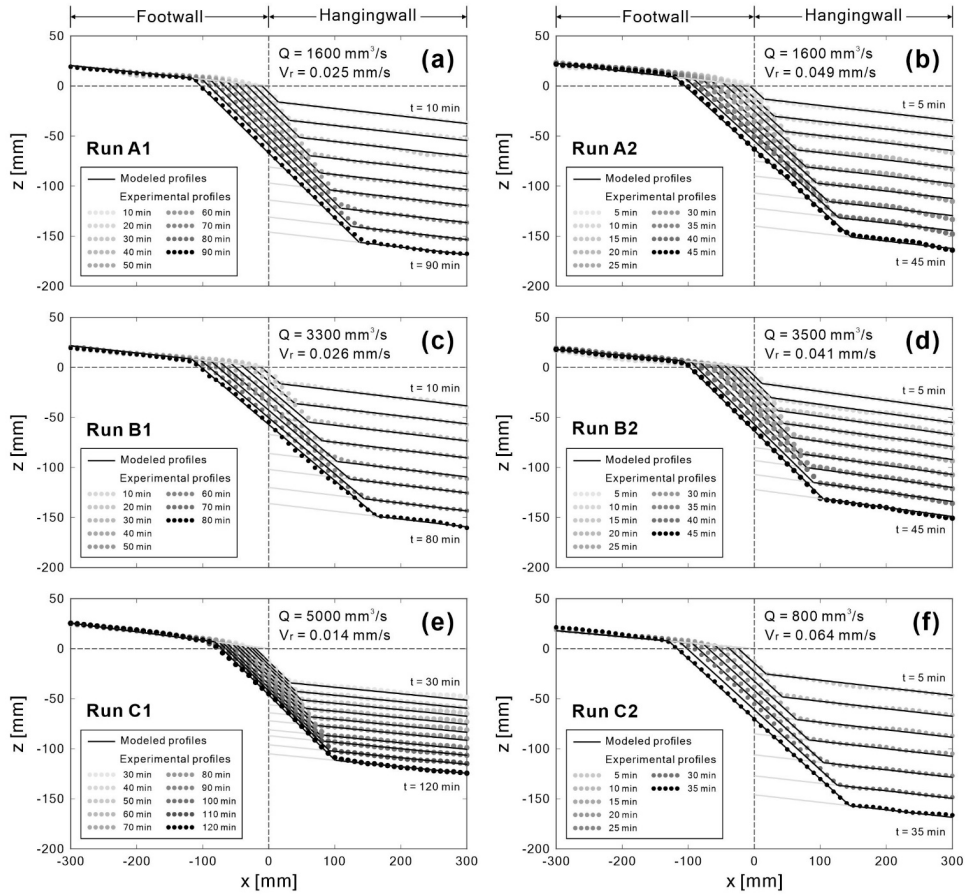
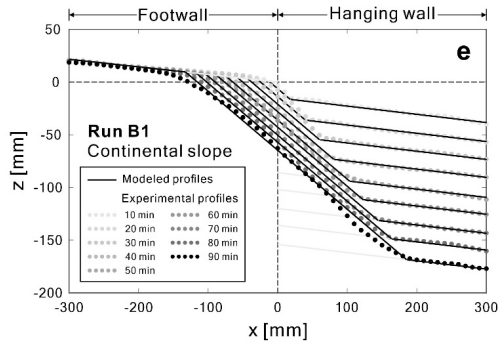


Figure 8. Comparisons between the experimental and simulated continental slopes in the different runs.

格式化: 定位停駐點: 不在 25.52 字元 + 46.78 字元



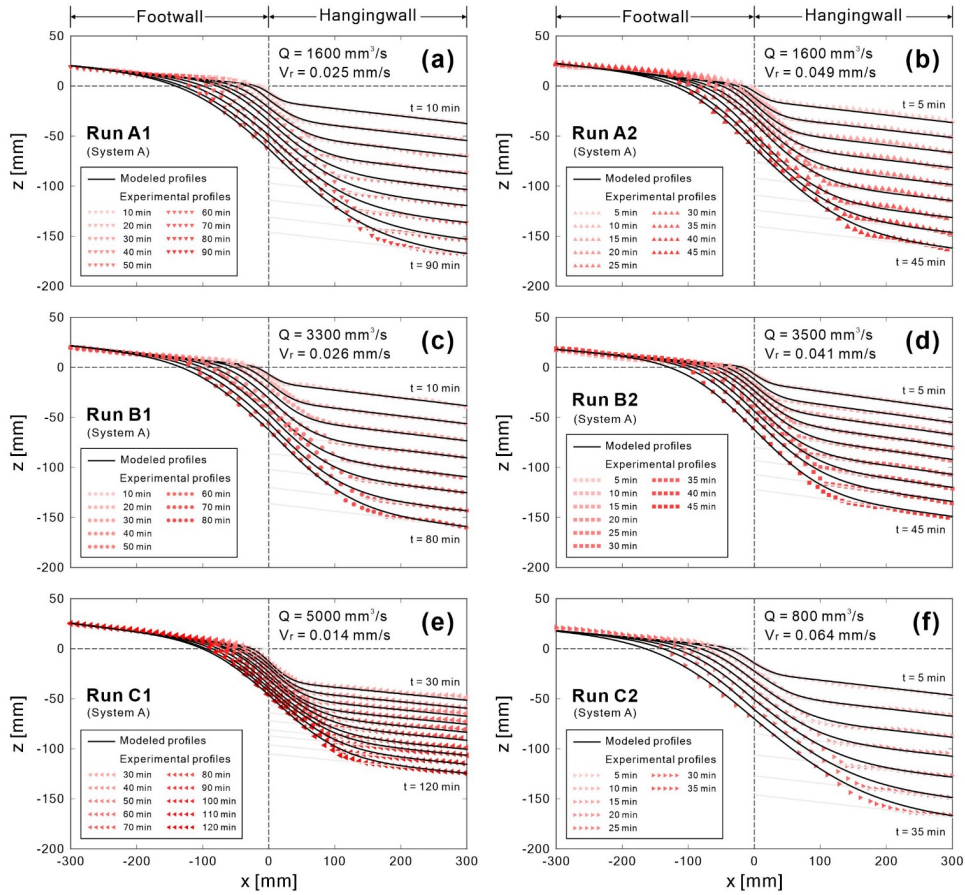


Figure 7.9 Comparisons between experimental and modeled-simulated submarine canyon-hangingwall fan long profiles in the different runs. (for Run B1). (a) to (d) Submarine canyon fan long profiles of the traced systems at different stages. (e) Continental slope long profiles traced at different stages. See Fig. S7 to Fig. S11 for long profile comparisons of other runs.

格式化: 字型: Times New Roman

格式化: 字型: Times New Roman

格式化: 字型: Times New Roman

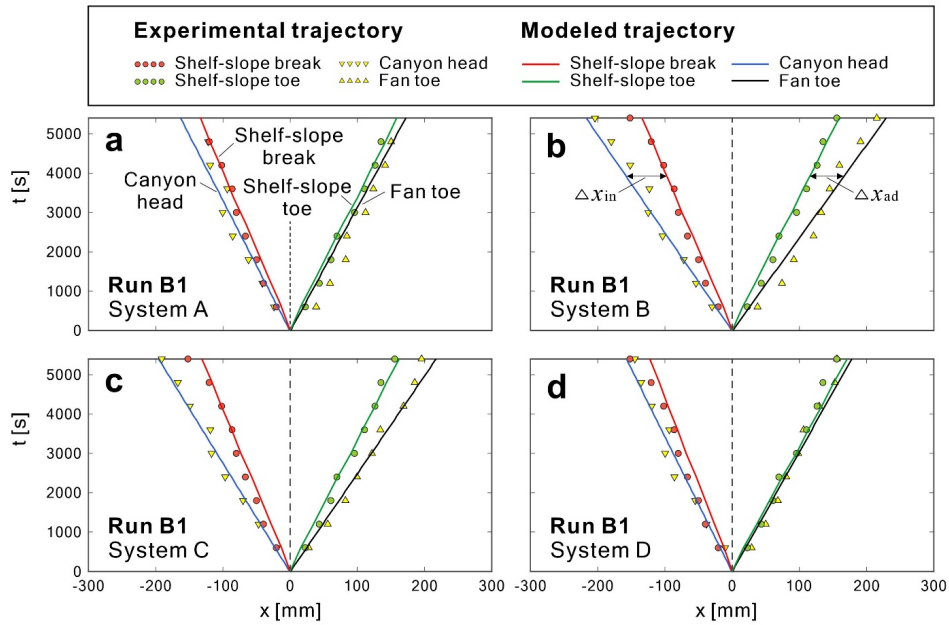
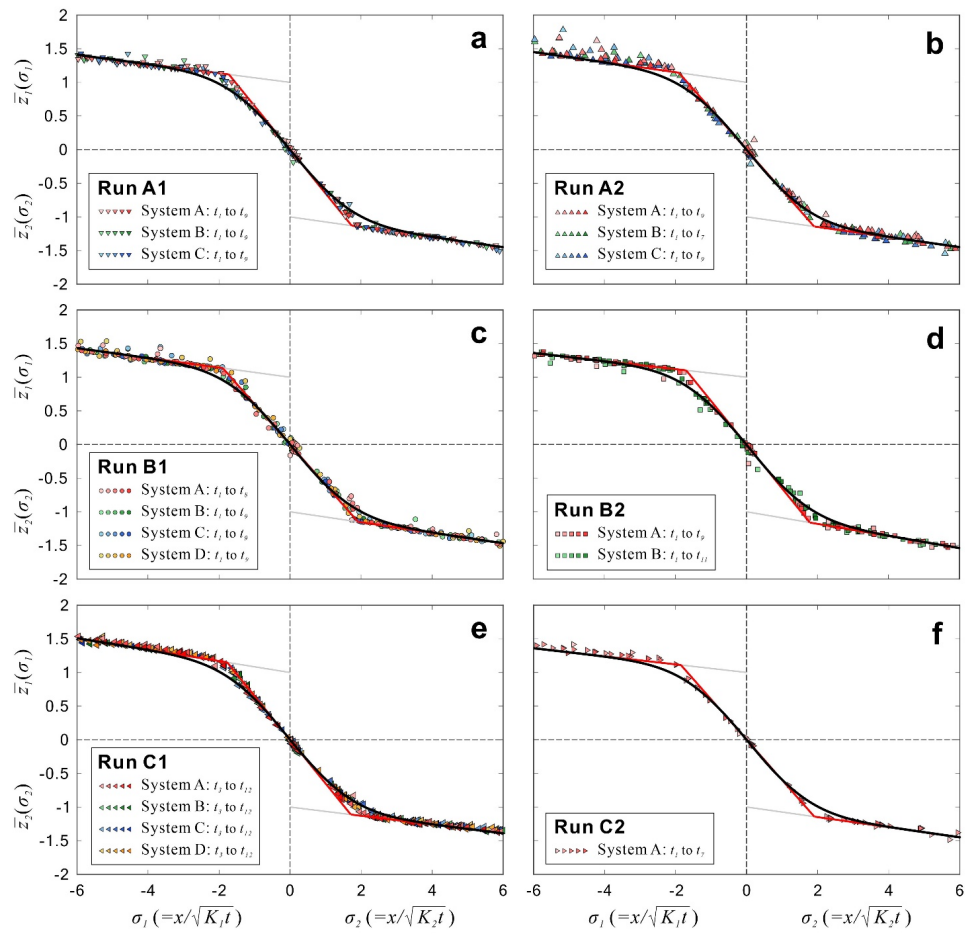


Figure 8. Comparison between experimental and modeled trajectories of the internal moving boundaries (for Run B1). The shelf slope break and shelf slope toe were extracted from the pseudo surface of each stage. Canyon incising distance (Δx_{in}) is the horizontal distance between the trajectory of canyon head to shelf slope break. Fan advancing distance (Δx_{ad}) is the horizontal distance between the trajectory of fan toe to shelf slope toe.

465



格式化: 置中

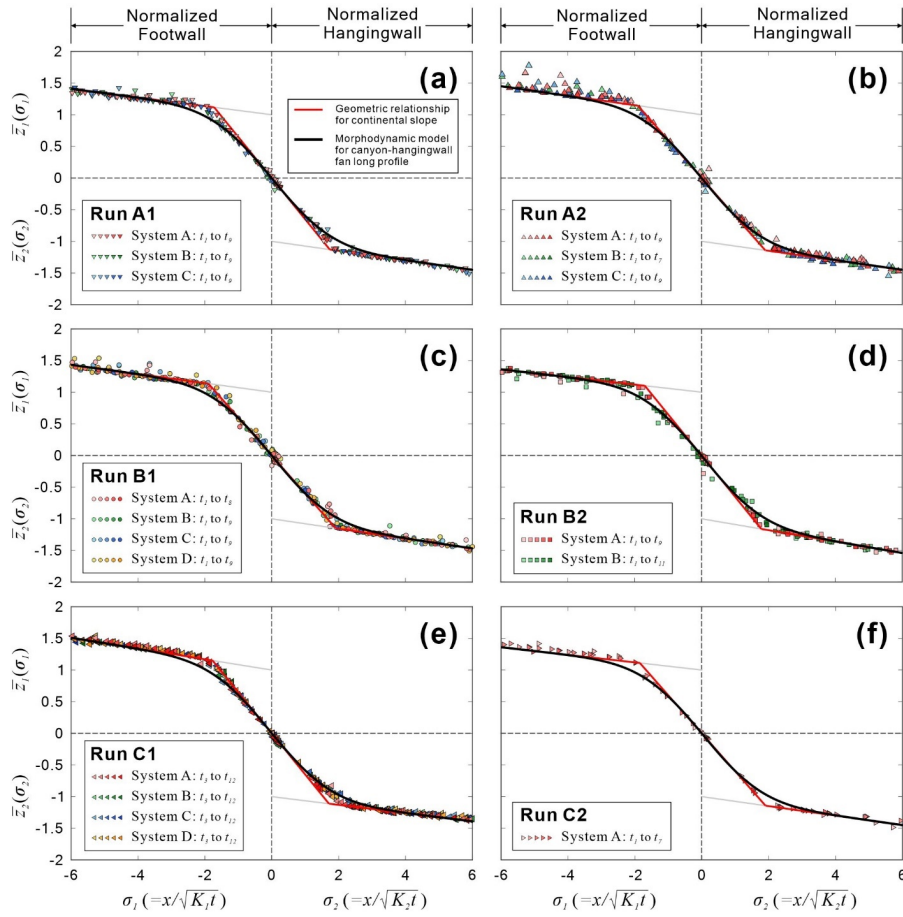


Figure 910. Dimensionless long profiles of for each run. Black solid lines are modeled dimensionless canyon-fan long profiles by two-diffusion theory. Red solid lines represent modeled dimensionless continental slopes. Gray solid lines show the normalized step function. Note that the numbers and times of each traced system are not identical.

470

475

3.3.4 Scaling relationships in-of submarine canyons and hangingwall-fans systems

The results of the morphometric analysis demonstrated that parameters in submarine canyons and hangingwall fans exhibit strong scaling relationships (Fig. 11). For instance, there is a significant linear correlation between canyon length (L_c) and canyon area (A_c), which aligns with Hack's empirical relationship (Fig. 11a). The Hack's coefficient is 1.75, and the exponent coefficient is 0.51. In hangingwall fans, we also observe a similar scaling relationship according to Hack's law between fan length (L_f) and fan area (A_f) (Fig. 11b). The Hack's coefficient is 1.3, and the exponent coefficient remains 0.51 as well. Moreover, combining the canyon relief height (H_1) and fan relief height (H_2), as determined by the morphodynamic model in Section 3.3, we propose empirical formulas for estimating the canyon volume (Ve_c) and the fan volume (Ve_f) using the area and relief height. These formulas are as follows: $Ve_c = \alpha \times H_1 \times A_c$, where α represents the experimentally calibrated coefficient ($\alpha = 0.1$ in this study), and $Ve_f = \beta \times H_2 \times A_f$, where β represents the experimentally calibrated coefficient ($\beta = 0.1$ in this study). The results demonstrate a close correspondence between the estimated canyon volume (Ve_c) and fan volume (Ve_f) using our proposed empirical formulas and the directly measured canyon volume (V_c) and fan volume (V_f) obtained from DoDs (Fig. 11c and Fig. 11d).

To validate the scaling relationship between length and area obtained from laboratory-scale, we compared the laboratory data with field data (Fig. 12). The obtained results show that the length to area relationship obtained from laboratory-scale submarine canyons and hangingwall fans is consistent with the field-scale submarine canyon length to fluvial drainage area analyzed in S2S studies ($n = 9477$, Harris and Whiteway, 2011). Our data also aligns with modern metadata of active margins ($n = 35$, Bührig et al., 2022a; 2022b) and passive margins ($n = 36$, Bührig et al., 2022a; Bührig et al., 2022b). Additionally, we find that this relationship ($L = 1.75 A^{0.51}$) also correlates well with the channel length to drainage area obtained from classic large fluvial rivers. For example: Tennessee Valley ($n = 63$, Montgomery and Dietrich, 1989); Linear mountain belt ($n = 193$, Hovius, 1996); Fault blocks ($n = 51$, Talling, 1997); 50 largest rivers ($n = 50$, Vörösmarty et al., 2000); Death Valley ($n = 18$, Bull, 1962; Denny, 1965); and even on Mars, this length to area relationship is maintained (Kraal et al., 2008). Moreover, the Hack's exponent falls within a reasonable range (0.46-0.56), e.g., the Hack's exponent is 1 for linear canyons and 0.5 for dendritic canyons of the Atlantic USA continental slope (Mitchell, 2005); the Hack's exponent is 0.46 for canyons in the south Ebro Margin (Micallef et al., 2014); the Hack's exponent is 0.49 for terrestrial river drainage basins (Montgomery and Dietrich, 1992). Interestingly, our submarine canyons and hangingwall fans show a striking similarity in scale to the experiments of coastal overwash morphology ($n = 96$, Lazarus, 2016), defined as the sedimentary deposit of microtidal barrier, as well as field-scale overwash (Hudock lobes, $n = 117$, Hudock et al., 2014; Core Bank, $n = 65$, Lazarus, 2016), all exhibiting the same scaling relationship. Therefore, the Hack's scaling relationship established from our evolving submarine canyons and hangingwall fans at the laboratory scale, spanning 22 orders and totalling 10784 data points, serves as an important link across submarine to terrestrial and laboratory-scale to field-scale domains.

格式化: 字型: (英文)Times New Roman

格式化: 字型: (英文)Times New Roman

格式化: 字型: (英文)Times New Roman

格式化: 字型: 非粗體

格式化: 字型: (英文)新細明體, (中文)新細明體, (中文)中文 (台灣)

格式化: 字型: 非粗體

格式化: 定位停駐點: 不在 25.52 字元 + 46.78 字元

格式化: 字型: 非粗體

格式化: 字型: 斜體

格式化: 字型: 斜體

格式化: 上標

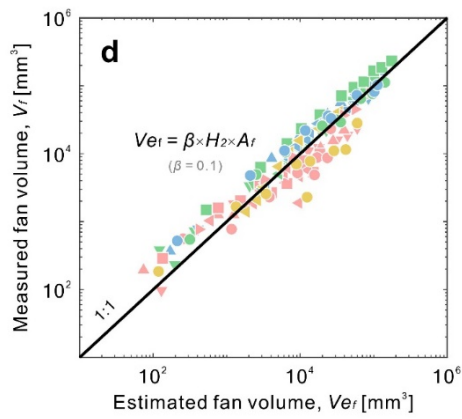
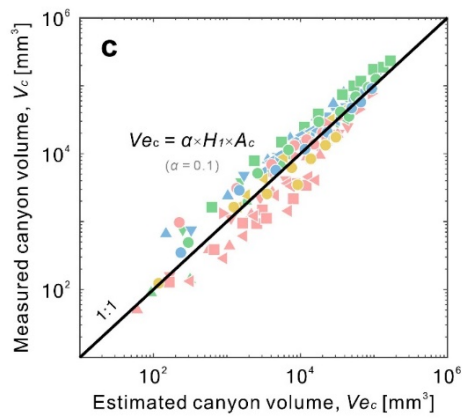
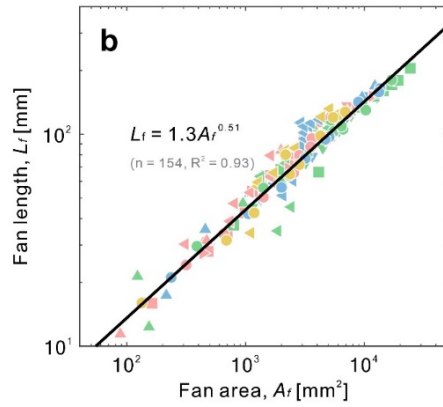
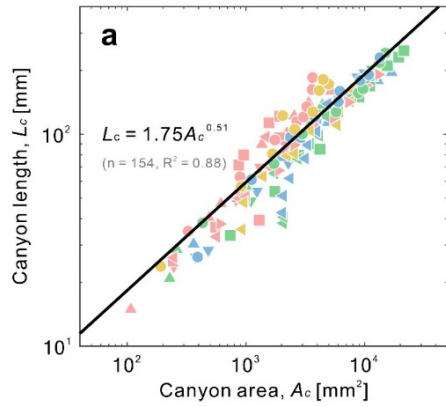
格式化: 字型: 非粗體

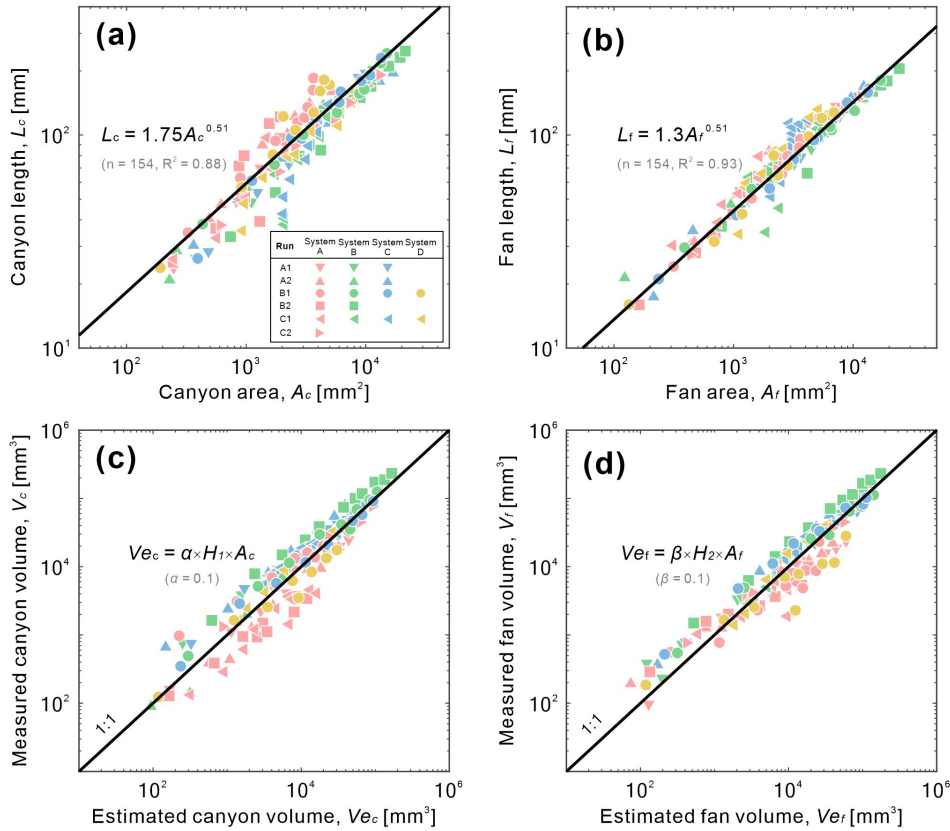
格式化: 字型: 非粗體

格式化: 字型: 非粗體

格式化: 字型: (英文)+本文 (Times New Roman), 英文 (美國)

Morphometric analyses showed that scaling relationships among submarine canyons and fans were robustly linear (Fig. 10). For instance, the experimental canyon lengths to canyon areas agreed with Hack's scaling relationship (Fig. 10a). Similarly, the scaling relationship was also established in experimental fan lengths to fan areas, with different Hack's coefficients but identical power (Fig. 10b). In addition, the canyon volume (V_c) can be estimated from upstream knickpoint height (H_u) and canyon area (A_c), following the formula $V_c = \alpha \times H_u \times A_c$, where α is a coefficient to be calibrated. Equivalently, the fan volume (V_f) followed $V_f = \beta \times H_d \times A_f$, where β is a coefficient to be calibrated. H_d is downstream knickpoint height. A_f is fan area. The results showed that the estimated volumes of canyons had a strong 1 to 1 relationship with the volumes measured directly from the DoDs, giving the coefficient $\alpha = 0.1$ (Fig. 10c). A similar trend was also established for submarine fans (Fig. 10d), making $\beta = 0.1$. These scaling relationships served as the basis for proposing a general rule by using canyon lengths to predict fan volumes, which will be explained in Section 4.





520

Figure 401. (a-b) The The Hack's length to area scaling relationships of length to area established for submarine canyons and fans, respectively. (c-d) 1 to 1 relationship for the estimated to measured volumes of canyons and fans, respectively.

525

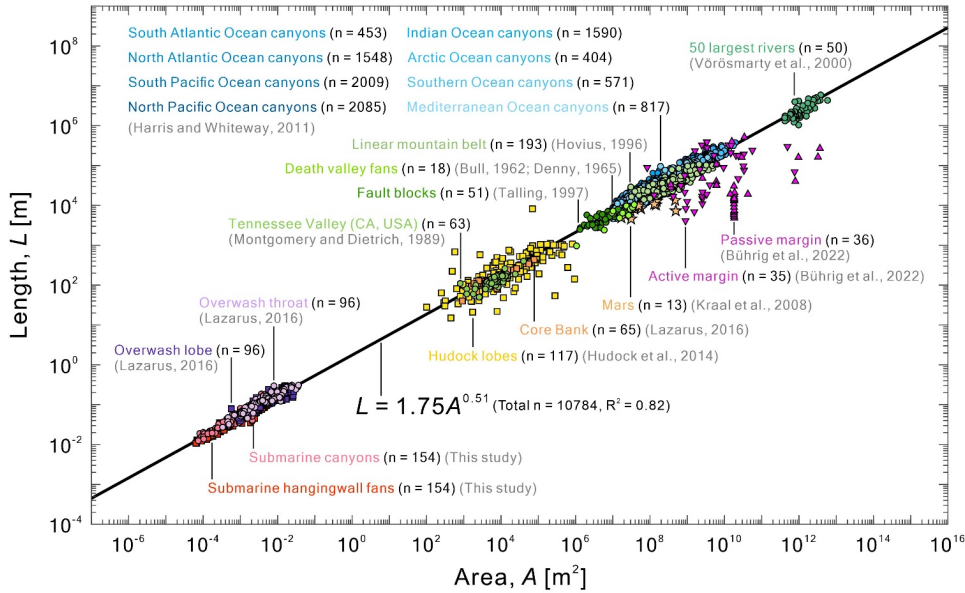


Figure 12. The length-to-area scaling relationship constructed from laboratory-scale to field-scale, with data from submarine canyons to terrestrial drainages.

4 Discussion

The main purpose of this study is to understand the response of submarine canyons and hangingwall fans to fault slip rate and inflow discharge through geomorphic experiments and morphodynamic models. We aim to establish scaling relationships across scales to help estimate volume information through canyon-fan evolution, which is difficult to obtain through classical geomorphic and stratigraphic studies. Below, we address three key issues that arise from our research. The purpose of this study is to understand the initiation and evolution of fault-controlled submarine canyon fan systems driven by downslope gravity flows. According to our experimental and modeling results, we propose that the morphological diversity of fault-controlled submarine canyon fan systems is controlled by fault slip rate and inflow discharge. Scaling relationships revealed

- 格式化: 字型: 粗體
- 格式化: 字型: Times New Roman, 粗體
- 格式化: 字型: 粗體
- 格式化: 字型: Times New Roman, 粗體
- 格式化: 字型: 粗體
- 格式化: 字型: (英文)Times New Roman, 粗體
- 格式化: 字型: 粗體
- 格式化: 字型: (英文)Times New Roman, 粗體
- 格式化: 字型: 粗體
- 格式化: 字型: (英文)Times New Roman, 粗體
- 格式化: 字型: Times New Roman
- 格式化: 字型: Times New Roman, 粗體
- 格式化: 字型: Times New Roman

545 in this study support us to establish a general rule for using canyon lengths to predict fan volumes, which greatly increases the applicability of the present work.

4.1 Why do geomorphic experiments work?

555 Geomorphic experiments are valuable tools for studying the processes and dynamics of landforms and landscapes. They involve manipulating physical variables in controlled environments to simulate natural conditions and understand their underlying mechanisms. By conducting these experiments, researchers can observe and measure how landforms and landscapes respond to factors like erosion, sediment transport, and deposition. These experiments provide valuable insights into the complex interactions between hydraulic, geomorphic, and sedimentological processes. Ultimately, researchers aim to identify self-similar laws or cross-scale relationships that exist within the system. In many cases, such experiments have proven feasible even for phenomena so far beyond the reach of numerical simulations.

560 For instance, in our experiments, we observed unprecedented evolution of submarine canyons and hangingwall fans, including the merging phenomenon between canyons and the coalescing process of fans (Fig. 4 and Fig. 5 and Fig. S1 to Fig. S6), and the formation of drainage networks in submarine canyons (Video S1 to Video S6). These are long-term landscape evolution features that cannot be observed in the field. In addition, we found that the long profiles extracted from our experiments exhibit a high degree of self-similarity (Fig. 10), indicating that they are scale versions of each other. Furthermore, in our morphometric analyses, we demonstrated that Hack's scaling relationship is an empirical formula applicable across laboratory to field scales from submarine to terrestrial systems (Fig. 12). These results all support the scale independence and applicability of our experimental results.

565 In our experiment, all morphologies occurring on the continental slope originate from fault slip-generated increasing relief. Submarine canyons and hangingwall fans only appear in areas where density underflows flow through. In regions without fault movement, such as the continental shelf in the footwall region (Fig. 4b), there will be no morphological changes, i.e., underflows will bypass the continental shelf until they encounter the shelf-slope break, where morphological changes will start to occur. This is one of the key elements in our experimental approach. This study aligns with the conclusion of Lai et al (2016) that the sustained formation of submarine canyons in the laboratory requires both increased relief and the presence of high-density underflows. We decouple this complex phenomenon into two main mechanisms: (1) breaching processes driven by gravity, including debris flows and mass wasting processes. At a laboratory scale, the morphological response is that the slope will maintain an angle of repose; and (2) submarine canyons and hangingwall fans formed by saline underflow incision, transport, and deposition. The underlying mechanisms we interpret are similar to the appearance of submarine hangingwall fans in syn-rift successions (McArthur et al., 2013; Barrett et al., 2021), which involves mixing of turbidity currents and mass-

575

格式化: 英文(美國)

wasting processes. We also agree that the volume of footwall-sourced hangingwall fans are comparable to the volume of material eroded from the fault scarp (Barrett et al., 2021).

580 However, there is a notable scarcity of geomorphic experiments focused on submarine canyon evolution. Our experimental approach diverges from that of Métivier et al. (2005) and Weill et al. (2014). Their experimental submarine canyons started from a given slope-to-plain condition, and they measured the evolution of submarine gullies and lobes at the slope break. These studies do not emphasize the potential influence of continuous active tectonics on the evolution of submarine canyons. Also, our experiments are different from those studies of submarine fan evolution (Cantelli et al., 2011; Fernandez et al., 2014; Ferguson et al., 2020), which were particularly designed to understand the sedimentary processes and stratigraphy formed by a point-source turbidity current on a ramp of constant-slope. These experiments neither emphasize the role of tectonics that may influence the evolution of submarine canyons and submarine fans. Our approach to generating evolving dynamic continental slopes is extended from Lai et al. (2016). They achieved the continuous effect of tectonics (i.e., increasing relief) by continuously lowering the base level to provide sufficient substrate for underflows to erode, thereby forming submarine canyon drainages that can evolve over time. This approach is similar to the subaerial experiments conducted by Hasbargen and Paola (2000) for simulating the evolution of drainage systems through rainfall erosion caused by base level fall. It is also similar to the subaerial experiments conducted by Strak et al. (2011) on normal faults, which resulted in the formation of valleys and alluvial fans. In addition, mountain building experiments generated by uplifting and rainfall (Bonnet and Crave, 2003, 2006; Babault et al., 2005) also support the hypothesis that controlling increasing relief is the key to generate dynamic drainage systems over time. Our experimental approach can be seen as an extension of fluvial drainage experiments, applied to subaqueous environments with a focus on tectonics and underflow driven deep-water sedimentary systems. Therefore, our current experimental approach for studying submarine canyons and hangingwall fans is unique.

600 To conclude, we reaffirm the findings of our prior research demonstrating that both increasing relief and sediment gravity flows are the two foundation factors for the progressive development of submarine canyons at laboratory scale. We also underscore the scale-independence and self-similarity on submarine canyon-hangingwall fan long profiles within our geomorphic experiments. Our experimental approach echoes the advantages of geomorphic experiments mentioned in Paola et al. (2009) and Lajeunesse et al. (2010), which have demonstrated to be valuable in validating numerical models and aiding in the interpretation of field cases. However, readers must exercise caution when interpreting field observations in light of our experimental results. Our experiments only consider fault slip rate and inflow discharge, which is highly simplified conditions. 605 Additionally, factors such as grain size, different tectonic processes, turbidity currents with fine suspended deposits, water salinity, temperature, ocean currents and other environmental factors may lead to experimental results may diverge from real-world field scenarios.

4.2 Fault slip rate and inflow discharge control the morphology of submarine canyons and hangingwall fans

We found that fault slip rate (V_r) has a greater control over the morphologies of submarine canyons and hangingwall fans compared to inflow discharge (Q), especially affecting the number and spacing of systems, as well as the volume of erosion and deposition. When the fault slip rate is higher, retrograding (or breaching) processes on the continental slope and canyon walls become more intense. Under the same flow rate, saline underflows need to converge in order to maintain canyon entrenchment on the continental slope, facilitating the piracy of contiguous canyons. On the contrary, when the fault slip rate is lower, even under high flow rates, the excess flow will bypass the slope, resulting in insignificant effects on the morphology and depth changes of submarine canyons. For example, in Run A2 (Fig. 6d), Run B2 (Fig. 6e), and Run C2 (Fig. 6f), a higher fault slip rate will result in a decrease in the number of submarine canyons and hangingwall fans, as well as a closer spacing between canyons. However, it will significantly increase the erosion volume of the submarine canyons (Fig. 7f). Our experimental results agree with the conclusion of Soutter et al., (2021b). The authors examined the factors controlling the concavity of submarine canyons by analyzing 377 modern canyons. Their results indicate that tectonics (similar to our fault slip rate condition) is the primary factor influencing concavity, with active margins having the least concave profiles. The position of the canyon and onshore climate (similar to our inflow discharge condition) also contribute, but to a lesser extent. In summary, our experimental results indicate that the fault slip rate (i.e., tectonic effects) have a greater control over the morphologies of submarine canyons and hangingwall fans compared to the inflow discharge (i.e., surface processes). Our conclusion is consistent with the conclusion of Soutter et al. (2021b), i.e., tectonics is the overriding control for deep-water sedimentary systems.

格式化: 定位停駐點: 不在 25.52 字元 + 46.78 字元

4.3 Canyon morphometrics to estimate submarine fans volume

First, we find that fault slip rates control the merging speed among canyon fan systems, which in turn affects the number and spacing of the system. A faster fault slip rate generates a greater fault escarpment, which resulted in a stronger retrograding process on the slope. This severer retrograding process facilitates the downslope gravity flows to converge, making the canyon fan systems to merge rapidly. For instance, under a fixed inflow discharge ($Q = 1600 \text{ mm}^3/\text{s}$), double the fault slip rate (Run A2), the number and spacing were much less than that of Run A1 (Fig. 5a and 5b). Similarly, under an increased inflow discharge ($Q = 3400 \text{ mm}^3/\text{s}$), double the fault slip rate (Run B2), the number and spacing is also much less than that of Run B1 (Fig. 5c and 5d). For the volume of canyon incision, the influence of fault slip rate is significant (Fig. 11a and Fig. 11b). The canyon incision volumes generated by faster fault slip rates is two times larger than that generated by a slower fault slip rate. Our experimental results agree with the idea that canyons in active margins are shorter, steeper, more dendritic and closely spaced (Harris and Whiteway, 2011). We further emphasize that in active margins the fault slip rate controls the merging speed, spacing and quantity of the submarine canyon fan systems.

格式化: 英文 (美國)

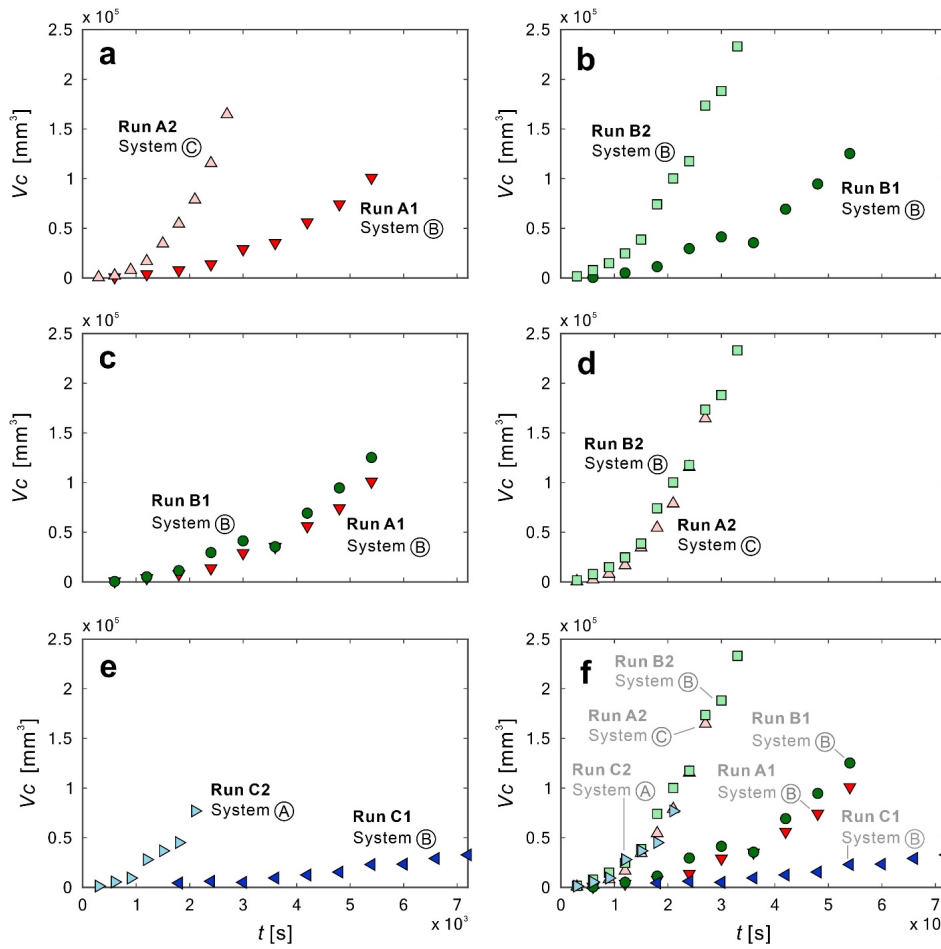
格式化: 字型: (中文) 新細明體, 非粗體, (中文) 中文 (台灣), (其他) 英文 (美國)

格式化: 標題 2, 定位停駐點: 不在 25.52 字元 + 46.78 字元

Second, the length, area and volume of canyons and fans is proportional to inflow discharge, but doubling the inflow discharge has minor influence on its morphology. Larger discharges cause stronger axial incision, triggered more retrograding landslides on canyon walls, and eventually increased the corresponding lengths, areas and volumes of the

645 systems. For instance, at a fixed fault slip rate (0.025 mm/s), double the inflow discharge (Run B1), the corresponding
size and number are similar to that of Run A1 (Fig. 5a and 5c). Similarly, at an increased fault slip rate (0.045 mm/s),
650 double the inflow discharge (Run B2), the size and numbers are also similar to that of Run A2 (Fig. 5b and 5d). For the
volumes of canyon incision, the influence of inflow discharge was insignificant than that of fault slip rate (Fig. 11c and
Fig. 11d). The canyon incision volumes generated by larger inflow discharge are slightly larger than that generated by
smaller inflow discharge. Our experimental results agree with that larger discharge forms deeper canyons (Weill et al.,

2014). However, we emphasized that the influences due to inflow discharge are insignificant when comparing to the morphological changes caused by fault slip rate.



格式化: 标题 2, 靠左, 定位停靠点: 不在 25.52 字节 + 46.78 字节

格式化: 西班文 (西班牙)

格式化: 字型: Times New Roman

格式化: 字型: Times New Roman

格式化: 标题 2

655 **Figure 11. Effects of fault slip rate and inflow discharge on the volume of evolving submarine canyons. (a-b) Influence of fault slip rate. (c-d) Influence of inflow discharge. (e) Influence of coupled fault slip rate and inflow discharge. (f)**

Comparison among all runs. All the selected systems were major shelf-incising canyons, except for Run C1, which belonged to slope-confined canyons.

格式化: 標題 2, 定位停駐點: 不在 25.52 字元 + 46.78 字元

Third, we believe that submarine canyon-fan systems react to coupled fault slip rate and inflow discharge is a competitive relationship, rather than a simple positive correlation. Extremely fast slip rate generates fault escarpment rapidly. Thus, if the inflow discharge is relatively small, the slope morphologies rapidly merge into a few major shelf-incising canyons. On the contrary, slow fault escarpment allow most of the inflow bypass the slope. The corresponding morphologies are slope-confined canyons. For instance, the slip rate of Run C2 is 5 times larger than that of Run C1, but the inflow discharge of Run C2 is only 1/6 than that of Run C1. The corresponding canyon lengths and volumes of Run C2 are 5-8 orders larger than those of Run C1 (Fig. 11e and Fig. 11f). Therefore, we propose that under the coupled effects of fault slip rate and inflow discharge, the final slope morphology is dominated by fault slip rate, rather than the inflow discharge.

Specifically, our experimental results may help to interpret the evolution of submarine canyon-fan systems observed on Haida Gwaii Trough. Although laboratory-scale to field-scale are 10^5 -order different, the morphological characteristics and fault settings suggest a similar formation for these two systems. The Haida Gwaii Trough is a bathymetric depression between Haida Gwaii Island and Queen Charlotte Terrace, similar to a graben between two normal faults, with different subsidence rates (~ 1 mm/yr to 3 mm/yr from north to south, estimated from Harris et al., 2014). Above the fault line, both types of canyons (shelf incising and slope-confined canyons) appear on the continental slope; below the fault line, a series of coalescing submarine fans are deposited on the Haida Gwaii Trough (Harris et al., 2014). These morphological characteristics and fault settings are similar to our experimental set-up and results. In addition, our experimental videos provide a way to visualize the evolution of merging canyons and coalescing fans that are rarely possible to observe in the field. Therefore, we believe that by isolating fault slip rate and inflow discharge it is possible to explain the origin and evolution of the submarine canyon-fan systems observed on Haida Gwaii Trough.

There have been several metadata studies (Somme et al., 2009; Nyberg et al., 2018; Bührig et al., 2022a; Bührig et al., 2022b) that have established the relationships between various parameters in S2S systems using morphometric analysis. However, correlating sediment volumes to canyon data analysis remains very limited, and the challenge of quantifying volume changes in submarine canyons and fans over long-term evolutionary processes persists. In Section 3.4, we revealed that Hack's scaling relationship ($L = 1.75 A^{0.51}$) can link the length to area relationship of both subaerial and subaqueous examples, with the area axis spanning across 22 orders of magnitude. Additionally, we also found in our experiments that canyon volumes can be estimated using canyon relief height and canyon area (Fig. 11c), and that fan volumes can be estimated using fan relief height and fan area (Fig. 11d). Therefore, we propose an empirical formula for estimating fan volume (V_f) in deep-water sedimentary systems using only the length of the submarine canyon (L_c). The formula is $L_c = 4.5 V_f^{0.33}$. This formula has been validated through our experiments and morphodynamic model (Fig. 13a), and does not require additional information from terrestrial drainages.

格式化: 字型: 斜體

格式化: 上標

695 To validate this formula, we compared 26 field cases from global databases that have both canyon length and fan volume
information (Somme et al., 2009 and references therein). These cases include 11 examples from passive margins, 10 examples
from small active margins, 2 examples from large active margins, and 3 examples from mixed margins. We found that the
estimated fan volumes using this formula align well with the observed data from these field cases (Figure 13b). In addition,
we estimated the corresponding fan volumes using 35 modern canyon length data from active margins and 36 modern canyon
700 length data from passive margins (Bührig et al., 2022; Bührig et al., 2022b). The estimated results align with the fan volumes
documented in past global datasets. However, further field data is required to validate the accuracy of these estimations. To
conclude, alongside Hack's scaling relationship, we propose a new empirical formula for estimating fan volumes using canyon
lengths. We anticipate that this formula will aid in estimating sediment volumes in deep-water sedimentary systems at their
terminus. However, it is important to approach the interpretation of this simple empirical formula with caution. For instance,
705 is may not be suitable for estimating the lobe elements generated in the distal part of a submarine channel (Prélat et al., 2010;
Pettinga et al., 2018). Additionally, complex tectonics, diverse flow conditions, and environmental factors can lead to
discrepancies between the estimated results and reality. Finally, we reveal the scaling relationships that link laboratory-scale
experiments with field-scale submarine canyon fan systems and we propose a general rule to predict fan volumes by simply
using canyon lengths. In field-scale submarine canyon fan systems, there are obvious limitations to obtain sediment
distributions over time and space. However, our experimental canyons and fans show strong Hack's scaling relationships with
710 the Hack's exponent of 0.51. Note that, for instance, the field-scale Hack's exponent is 1 for the linear canyons and 0.5 for the
dendritic canyons on the Atlantic USA continental slope (Mitchell, 2005); 0.46 for the canyons in the south Ebro Margin
(Micallef et al., 2014b); 0.49 for the terrestrial river drainage basins (Montgomery and Dietrich, 1992). Combining the Hack's
scaling relationship of canyons (Fig. 10a) and the strong 1:1 relationship of measured to estimated fan volumes (Fig. 10d), we
propose a general rule by using canyon lengths to predict fan volumes:

$$L_c = 4.5 \cdot V_f^{0.33} \quad (5)$$

where L_c = canyon length; V_f = fan volume. This formula is verified by our morphodynamic model (Fig. 12a). We keep this
verified relationship and compare our experimental data to 26 global source-to-sink systems (Somme et al., 2009) (Fig. 12b).
We find that this formula is applicable to all observed canyon fan systems in different margins (passive, mixed and active
720 margins). The reason is that the evolution of submarine canyons is mainly controlled by increasing reliefs and downslope
gravity flows (Lai et al., 2016). Active margin (through tectonic shortening) or passive margin (by prograding sedimentation
over a deep basin) are different ways to generate increasing reliefs. The effect is to steepen the continental slope, resulting in
local oversteepening. When the inflow discharge is fixed, the steepening of the bed slope will increase the dimensionless
stream power and the sediment transport capability of downslope gravity flows (Lai et al., 2017), i.e., increasing relief is to
725 allow the gravity flows to obtain higher potential energy, which is then converted into stronger downslope kinetic
energy. Therefore, we think our experimental approach is universal for all margin types and Eq. (5) is a general rule, which
spans more than 20 orders from laboratory-scale to margin-scale. These results imply that our experiments are scale

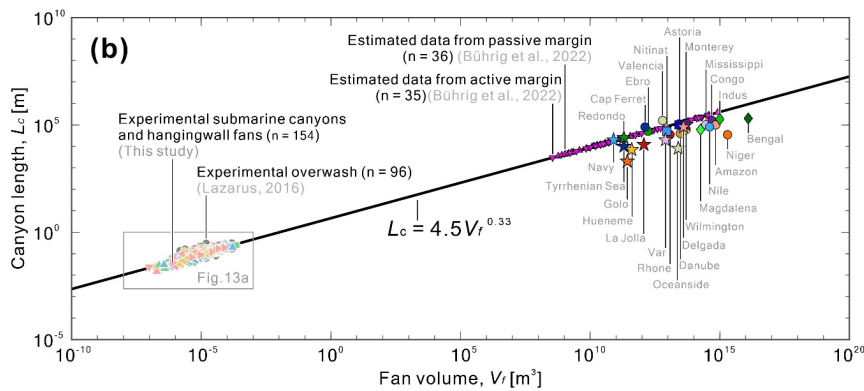
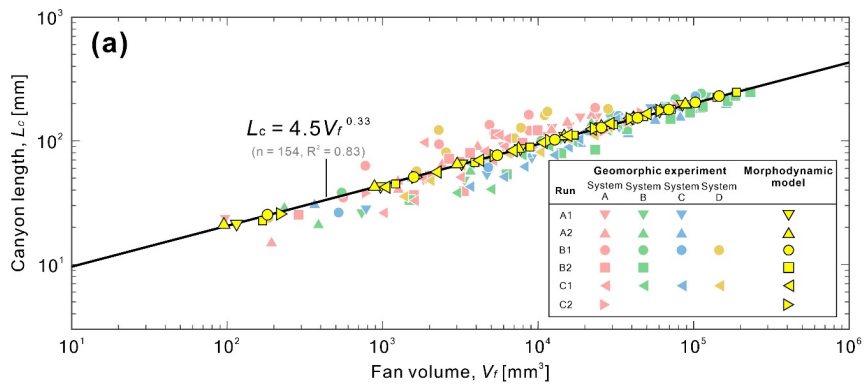
格式化: 字型: Times New Roman

independent, similar to other small-scale physical experiments (Paola et al., 2009; Lajeunesse et al., 2010; Lazarus, 2016). By applying Eq. (5) to the canyon-fan systems observed on Haida Gwaii Trough (Fig. 1a), considering that the length of the shelf-incising canyon is 12,000 m, the corresponding fan volume should be $24 \times 10^9 \text{ m}^3$; if the length of slope-confined canyon is 6,000 m, the fan volume should be $29.5 \times 10^8 \text{ m}^3$. Therefore, this general rule allows researchers to quickly use canyon lengths to estimate the first-order fan volumes, greatly improving the value and applicability of this study. It is worth to mention that our approach may not be applicable to the scaling relationships between lobes and lobe elements (Pettinga et al., 2018), which focused on the distal part of fan lobes.

730

735

格式化: 字型: Times New Roman



Passive margin (Sømme et al., 2009 and references therein)	Small active margin (Sømme et al., 2009 and references therein)	Large active margin (Sømme et al., 2009 and references therein)	Mixed margin (Sømme et al., 2009 and references therein)
○ Mississippi	☆ Var	■ Astoria	◆ Bengal
● Congo	★ Monterey	■ Niinat	◆ Indus
● Amazon	★ Delgada		◆ Magdalena
● Rhone	★ La Jolla		
● Valencia	★ Oceanside		
● Ebro	★ Redondo		
● Nile	★ Navy		
● Cap Ferret	★ Tyrrhenian Sea		
● Wilmington	★ Hueneme		
● Niger	★ Golo		
● Danube			
		Estimated data	
		▼ Estimated data from active margin (Bührig et al., 2022)	
		▲ Estimated data from passive margin (Bührig et al., 2022)	
		Other experimental data	
		● Experimental overwash (Lazarus, 2016)	

格式化: 置中

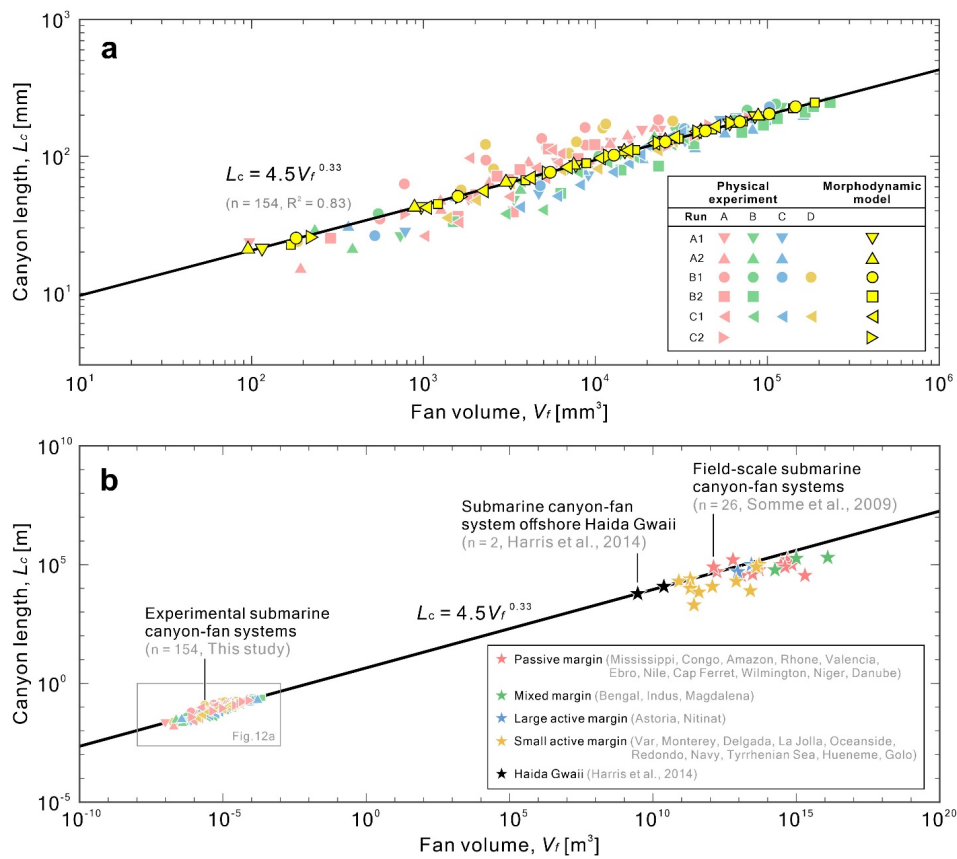


Figure 12.13. (a) The scaling relationship built from our experimental data and verified by the morphodynamic model. (b) The general scaling relationship of canyon lengths to fan volumes among laboratory-scale ($n = 154$, this study), margin-scale ($n = 26$, Somme et al., 2009), and offshore Haida Gwaii ($n = 2$, Harris et al., 2014).

740

5 Conclusions

745 In this paper, we propose a novel experimental approach to investigate the long-term geomorphic evolution processes of submarine canyons and hangingwall fans that are simultaneously influenced by tectonics and surface flows. Through physical experiments, morphometric analysis, and morphodynamic modelling, we have gained insights into the response of submarine canyons and hangingwall fans to fault slip rate (V_f) and inflow discharge (Q). We further presented scaling relationships that span from laboratory to field scales and from submarine canyons to terrestrial drainages. The following are our major findings:
750 Physical experiments and morphodynamic model allow us to better understand the responses of submarine canyon fan systems to fault slip rates and inflow discharges. The proposed general rule is ready to be applied to field-scale submarine canyon fan systems. Here are our conclusions:-

- 755 1. The experimental results show that fault slip rate controls the merging speed of submarine canyons and hangingwall fans, thereby affecting their quantity and spacing. Compared to inflow discharge, fault slip rate has a more dominant influence on submarine canyons and hangingwall fans and directly affects their volume. This conclusion is consistent with the overriding control of tectonics concluded from recent works on natural systems (e.g., Bernhardt and Schwanghart, 2021; Bührig et al., 2022a; Bührig et al., 2022b; McArthur et al., 2022; and Soutter et al., 2021b).
2. The long profile shapes of submarine canyons and hangingwall fans can be decoupled into gravity-dominated breaching processes and underflow-dominated diffusion processes, which can be described by a constant-slope relationship and a morphodynamic diffusion model, respectively.
3. The comparison between the experimental long profiles and our proposed constant-slope relationship and morphodynamic model shows a good agreement. Moreover, the long profiles of submarine canyons and hangingwall fans exhibit strong self-similarity, indicating their scale independence.
4. The Hack's scaling relationship established through morphometric analyses is a robust relationship spanning 22 orders of magnitude and over 10,000 data points. This relationship is built upon laboratory-scale data to field-scale data and serves as an important link between different scales in source-to-sink systems.
- 760 5. For deep-water sedimentary systems, we propose an empirical formula to estimate fan volume based on canyon length. This formula shows good agreement with the comparison results from 26 representative source-to-sink systems worldwide. We also estimate fan volumes for recent data from active margin and passive margin (Bührig et al., 2022a; Bührig et al., 2022b), which fall within a reasonable range compared to the globally representative fan volumes in source-to-sink systems.

775 However, we do not claim that the submarine canyons and hangingwall fans in our experiments are precise dynamical models of their field counterparts. Field examples result from complex, varied tectonic processes and underflow conditions, which may lead to significant discrepancies between the experiments and field cases. Therefore, when using our empirical formulas for interpretations, careful consideration of various tectonics and flow conditions for the specific field case is necessary. In

格式化: 字型: Times New Roman

780 addition, in the analysis of morphometric analysis, we did obtain data on canyon width and fan width. However, we have not yet discovered any interesting trends that can be compared to published data or help us predict hard-to-obtain volume information. Future research can continue to analyze these width data and perhaps establish more valuable relationships. In summary, our physical experiments provide a novel perspective to examine the long-term evolution processes of submarine canyons and hangingwall fans. The proposed empirical formula may help field researchers estimate volume information from incomplete bathymetric and stratigraphic data.

1. The results of morphometric analyses support that Hack's scaling relationships exist in both laboratory-scale and field scale submarine canyon fan systems.
- 785 2. The DEM of differences (DoDs) demonstrate the patterns of sediment erosion and deposition and provide reliable volumes of canyons and fans.
3. The validated submarine canyon fan long profiles show strong self-similarities. The corresponding trajectory of internal moving boundaries over time are surprisingly linear.
4. We propose that fault slip rate controls the convergence and merging speed of submarine canyon fan systems, which in turn affects their number and spacing.
- 790 5. At a fixed fault slip rate, the lengths, areas and volumes of canyons and fans are proportional to inflow discharge.
6. When considering coupled fault slip rates and inflow discharges, the influence of these two parameters to canyon fan morphology is a competitive relationship.
7. Finally, we unveil scaling relationships across laboratory to field scales and propose a general rule to predict fan volumes by using canyon lengths.
- 795

We assume that the morphodynamic processes causing the evolution of experimental submarine canyon fan systems may differ from the field analogues, but we claim and demonstrate that at least we are able to predict the first-order general morphological and sedimentological patterns at basin scale. In short, our findings are inspiring and valuable for field researchers and/or modelers to better interpret and predict the morphological evolution and sedimentary processes of submarine canyon fan systems in active fault settings. Next steps will be to consider different fault dip angles and even to explore thrust fault controlled submarine canyon fan systems in active convergent margins.

800

Data Availability

Data ~~is~~ are available at <http://doi.org/10.5281/zenodo.7271139>; ~~https://zenodo.org/record/7271139#~~ <https://zenodo.org/record/7271139#>. Y2MEQ3ZBxD8

功能變數代碼變更

Supplement

805 The supplement related to this article is available online at; <https://doi.org/10.5194/esurf-8-37-2020-supplement>.

格式化: 字型: Times New Roman

Author contributions

SYJL conceived the idea, performed the experiment and conducted the analysis. SYJL drafted the paper, with contributions from DA, AM, TPG and HC. All authors worked on the submitted final version.

Competing interests

810 The authors declare that they have no conflicts of interest.

Acknowledgements

815 ~~This study has been supported by the Ministry of Science and Technology (MOST), Taiwan (grant no. MOST 109-2628-E-006-006-MY3) and the National Science and Technology Council (NSTC), Taiwan (grant no. NSTC 112-2628-E-006-009-MY3). This study was supported by the Ministry of Science and Technology (MOST), Taiwan (grants to S. Y. J. L.: MOST 109-2628-E-006-006-MY3). We thank Jyun-Fong Jiang for helping with the design of the first version of the experimental tank. Students of the Morphohydraulics Imaging Laboratory (MIL), students Jyun-Fong Jiang, Sam Yan Jyun Huang, and Te-Min Kong provided valuable assistant during the performance the experiments. Students of Morphohydraulics Imaging Laboratory (MIL) are also well acknowledged for their help during the experiment runs. D.A. acknowledges-acknowledged~~
820 ~~the support from the Spanish government through the grants PID2020-114322RBI00 and EIN2020-112179 funded by MCIN/AEI/10.13039/501100011033 and NextGenerationEU, and the Catalan Government Excellence Research Groups Grant to GRC Geociències Marines (ref. 2017-2021-SGR-34501195). Thomas P. Gerber and Peter T. Harris were acknowledged for the early discussion on this research and providing global bathymetric data of submarine canyons, respectively.~~

格式化: 行距: 1.5 倍行高, 定位停駐點: 不在 25.52 字元 + 46.78 字元

格式化: 英文(美國)

Financial support

825 ~~This study was supported by the Ministry of Science and Technology (MOST), Taiwan (grants to S. Y. J. L.: MOST 109-2628-E-006-006-MY3). This study has been supported by the National Science and Technology Council (NSTC), Taiwan (grant no. NSTC 112-2628-E-006-009-MY3).~~ -

References

~~Ambias, D. and Dowdeswell, J.: Physiographic influences on dense shelf water cascading down the Antarctic continental slope, Earth Sci. Rev., 185, 887-900, 2018.~~

格式化: 縮排: 左: 0 公分, 第一行: 0 公分

830

Ambias, D., Gerber, T. P., Canals, M., Pratson, L. F., Urgeles, R., Lastras, G., and Calafat, A. M.: Transient erosion in the Valencia Trough turbidite systems, NW Mediterranean Basin, *Geomorphology*, 130, 173-184, DOI 10.1016/j.geomorph.2011.03.013, 2011.

835

Ambias, D., Gerber, T. P., Mol, B., Urgeles, R., Garcia Castellanos, D., Canals, M., Pratson, L. F., Robb, N., and Canning, J.: Survival of a submarine canyon during long-term outbuilding of a continental margin, *Geology*, 40, 543-546, Doi 10.1130/G33478.1, 2012.
Babault, J., Bonnet, S., Crave, A., and Van Den Driessche, J.: Influence of piedmont sedimentation on erosion dynamics of an uplifting landscape: An experimental approach, *Geology*, 33, 301, 10.1130/g21095.1, <https://doi.org/10.1130/G21095.1>, 2005.

840

Barrett, B. J., Hodgson, D. M., Jackson, C. A. L., Lloyd, C., Casagrande, J., and Collier, R. E. L.: Quantitative analysis of a footwall-scarp degradation complex and syn-rift stratigraphic architecture, Exmouth Plateau, NW Shelf, offshore Australia, *Basin Res.*, 33, 1135-1169, <https://doi.org/10.1111/bre.12508>, 2021.

845

Bernhardt, A. and Schwanghart, W.: Where and why do submarine canyons remain connected to the shore during sea-level rise? Insights from global topographic analysis and Bayesian regression, *Geophys. Res. Lett.*, 48, e2020GL092234, <https://doi.org/10.1029/2020GL092234>, 2021.
Barrie, J. V., Conway, K. W., and Harris, P. T.: The Queen Charlotte Fault, British Columbia: seafloor anatomy of a transform fault and its influence on sediment processes, *Geo-Mar. Lett.*, 33, 311-318, 10.1007/s00367-013-0333-3, 2013.

850

Bonnet, S. and Crave, A.: Landscape response to climate change: Insights from experimental modeling and implications for tectonic versus climatic uplift of topography, *Geology*, 31, 123-126, [https://doi.org/10.1130/0091-7613\(2003\)031<0123:LRTCCI>2.0.CO;2](https://doi.org/10.1130/0091-7613(2003)031<0123:LRTCCI>2.0.CO;2), 2003.

Bonnet, S. and Crave, A.: Macroscale dynamics of experimental landscapes, analogue and numerical modeling of crustal-scale processes, Special Publications, Geological Society, London, 2006.

855

Bourget, J., Zaragosi, S., Ellouz-Zimmermann, N., Mouchot, N., Garlan, T., Schneider, J.-L., Lanfumey, V., and Lallemand, S.: Turbidite system architecture and sedimentary processes along topographically complex slopes: the Makran convergent margin, *Sedimentology*, 58, 376-406, <https://doi.org/10.1111/j.1365-3091.2010.01168.x>, 2011.

Brothers, D. S., Uri, S., Andrews, B. D., Chaytor, J. D., and Twichell, D. C.: Geomorphic process fingerprints in submarine canyons, *Mar. Geol.*, 337, 53-66, 2013.

860

Bührig, L. H., Colomera, L., Patacci, M., Mountney, N. P., and McCaffrey, W. D.: Tectonic influence on the geomorphology of submarine canyons: implications for deep-water sedimentary systems, *Source or Sink? Erosional and Depositional Signatures of Tectonic Activity in Deep-Sea Sedimentary Systems*, <https://doi.org/10.3389/feart.2022.836823>, 2022a.

Bührig, L. H., Colomera, L., Patacci, M., Mountney, N. P., and McCaffrey, W. D.: A global analysis of controls on submarine-canyon geomorphology, *Earth-Sci. Rev.*, 104150, <https://doi.org/10.1016/j.earscirev.2022.104150>, 2022b.

865

Bull, W. B.: Relations of alluvial fan size and slope to drainage basin size and lithology in western Fresno County, California, *US Geological Survey Professional Paper*, 450, 51-53, 1962.

Canals, M., Puig, P., de Madron, X. D., Heussner, S., Palanques, A., and Fabres, J.: Flushing submarine canyons, *Nature*, 444, 354-357, 10.1038/nature05271, 2006.

870

Cantelli, A., Pirmez, C., Johnson, S., and Parker, G.: Morphodynamic and stratigraphic evolution of self-channelized subaqueous fans emplaced by turbidity currents, *J. Sediment. Res.*, 81, 233-247, <https://doi.org/10.2110/jsr.2011.2010.2110/jsr.2011.20>, 2011.

格式化: 標題 1, 縮排: 左: 0 公分, 第一行: 0 公分, 行距: 單行間距, 定位停駐點: 不在 25.52 字元 + 46.78 字元

格式化: 靠左

- Capart, H., Bellal, M., and Young, D. L.: Self-similar evolution of semi-infinite alluvial channels with moving boundaries, *J. Sediment. Res.*, 77, 13-22, <https://doi.org/10.2110/jsr.2007.009+0.2110/jsr.2007.009>, 2007.
- 875 Covault, J. A., Fildani, A., Romans, B. W., and McHargue, T.: The natural range of submarine canyon-and-channel longitudinal profiles, *Geosphere*, 7, 313-332, <https://doi.org/10.1130/GES00610.1> Doi:10.1130/Ges00610.1, 2011.
- [Denny, C. S.: Alluvial fans in the Death Valley region, California and Nevada, 466, US Government Printing Office 1965.](#)
- [Dadson, S., Hovius, N., Pegg, S., Dade, W. B., Horng, M. J., and Chen, H.: Hyperpycnal river flows from an active mountain belt, *J. Geophys. Res.: Earth Surf.*, 110, 2005.](#)
- 880 Fernandez, R. L., Cantelli, A., Pirmez, C., Sequeiros, O., and Parker, G.: Growth patterns of subaqueous depositional channel lobe systems developed over a basement with a downdip break in slope: Laboratory experiments, *J. Sediment. Res.*, 84, 168-182, <https://doi.org/10.2110/jsr.2014.10.168+0.2110/jsr.2014.10>, 2014.
- Foreman, B. Z., Lai, S. Y. J., Komatsu, Y., and Paola, C.: Braiding of submarine channels controlled by aspect ratio similar to rivers, *Nat. Geosci.*, 8, 700-703, <https://doi.org/10.1038/ngeo2505> 10.1038/NGEO2505, 2015.
- 885 [Ferguson, R. A., Kane, I. A., Eggenhuisen, J. T., Pohl, F., Tilston, M., Spychala, Y. T., and Brunt, R. L.: Entangled external and internal controls on submarine fan evolution: an experimental perspective, *Depos. Rec.*, 6, 605-624, <https://doi.org/10.1002/dep2.109>, 2020.](#)
- [Gamberi, F., Rovere, M., Marani, M. P., and Dijkstra, M.: Modern submarine canyon feeder system and deep-sea fan growth in a tectonically active margin \(northern Sicily\), *Geosphere*, 11, 307-319, 10.1130/Ges01030.1, 2015.](#)
- 890 Gerber, T. P., Ambias, D., Wolinsky, M. A., Pratson, L. F., and Canals, M.: A model for the long-profile shape of submarine canyons, *J. Geophys. Res.: Earth Surf.*, 114, ArtId F03002 Doi:10.1029/2008jff001190, 2009.
- [Haek, J. T.: Studies of longitudinal stream profiles in Virginia and Maryland, US Government Printing Office, 1957.](#)
- Hanks, T. C., Bucknam, R. C., Lajoie, K. R., and Wallace, R. E.: Modification of wave-cut and faulting-controlled landforms, *J. Geophys. Res.: Solid Earth*, 89, 5771-5790, <https://doi.org/10.1029/JB089iB07p05771>, 1984.
- 895 [Harris, P. T., Macmillan-Lawler, M., Rupp, J., and Baker, E. K.: Geomorphology of the oceans, *Mar. Geol.*, 352, 4-24, <https://doi.org/10.1016/j.margeo.2014.01.011>, 2014.](#)
- Harris, P. T. and Whiteway, T.: Global distribution of large submarine canyons: gGeomorphic differences between active and passive continental margins, *Mar. Geol.*, 285, 69-86, <https://doi.org/10.1016/j.margeo.2011.05.008>, 2011.
- 900 [Harris, P. T., Barrie, J. V., Conway, K. W., and Greene, H. G.: Hanging canyons of Haida Gwaii, British Columbia, Canada: Fault control on submarine canyon geomorphology along active continental margins, *Deep Sea Res. Part II*, 104, 83-92, 10.1016/j.dsr2.2013.06.017, 2014.](#)
- Hasbargen, L. E. and Paola, C.: Landscape instability in an experimental drainage basin, *Geology*, 28, 1067-1070, [https://doi.org/10.1130/0091-7613\(2000\)28<1067:LHAED>2.0.CO;2](https://doi.org/10.1130/0091-7613(2000)28<1067:LHAED>2.0.CO;2), 2000.
- 905 [Hovius, N.: Regular spacing of drainage outlets from linear mountain belts, *Basin Res.*, 8, 29-44, <https://doi.org/10.1111/j.1365-2117.1996.tb00113.x>, 1996.](#)
- [Lai, S. Y., Hung, S. S., Foreman, B. Z., Limaye, A. B., Grimaud, J. L., and Paola, C.: Stream power controls the braiding intensity of submarine channels similarly to rivers, *Geophys. Res. Lett.*, 44, 5062-5070, <https://doi.org/10.1002/2017GL072964>, 2017.](#)
- 910 [Horton, R. E.: Erosional development of streams and their drainage basins; hydrophysical approach to quantitative morphology, *Geol. Soc. Am. Bull.*, 56, 275-370, 1945.](#)
- [Hsieh, Y. h., Liu, C. s., Suppe, J., Byrne, T. B., and Lallemand, S.: The chimei submarine canyon and fan: A record of Taiwan arc-continent collision on the rapidly-deforming overriding plate, *Tectonics*, 39, e2020TC006148, 2020.](#)
- 915 [Lai, S. Y. J., Samuel S. C. Hung, Brady Z. Foreman, Ajay B. Limaye, and Jean-Louis Grimaud, a. C. P.: Stream power controls the braiding intensity of submarine channels similarly to rivers, *Geophys. Res. Lett.*, 10.1002/, 2017.](#)

格式化: 靠左, 缩排: 左: 0 公分, 第一行: 0 公分

格式化: 靠左

格式化: 字型: (英文)Times New Roman

格式化: 字型: Times New Roman

格式化: 第一行: -2.83 字元

格式化: 靠左, 第一行: -2.83 字元

格式化: 靠左

格式化: 靠左

格式化: 字型: Times New Roman

- Lai, S. Y. J. and Wu, F. C.: Two-stage transition from Gilbert to hyperpycnal delta in reservoir, *Geophys. Res. Lett.*, 48, [e2021GL093661](https://doi.org/10.1029/2021GL093661), <https://doi.org/10.1029/2021GL093661>, 2021.
- Lai, S. Y. J., Gerber, T. P., and Amblas, D.: An experimental approach to submarine canyon evolution, *Geophys. Res. Lett.*, 43, 2741-2747, <https://doi.org/10.1002/2015GL067376>, 2016.
- 920 Lajeunesse, E., Malverti, L., Lancien, P., Armstrong, L., Metivier, F., Coleman, S., Smith, C. E., Davies, T., Cantelli, A., and Parker, G.: Fluvial and submarine morphodynamics of laminar and near-laminar flows: a synthesis, *Sedimentology*, 57, 1-26, <https://doi.org/10.1111/j.1365-3091.2009.01109.x> DOI:10.1111/j.1365-3091.2009.01109.x, 2010.
- Lazarus, E. D.: Scaling laws for coastal overwash morphology, *Geophys. Res. Lett.*, 43, 12,113-142,119, <https://doi.org/10.1002/2016GL071213> DOI:10.1002/2016gl071213, 2016.
- 925 Leeder, M. and Gawthorpe, R.: Sedimentary models for extensional tilt-block/half-graben basins, Geological Society, London, Special Publications, 28, 139-152, 1987.
- Lo Iacono, C., Sulli, A., and Agate, M.: Submarine canyons of north-western Sicily (Southern Tyrrhenian Sea): Variability in morphology, sedimentary processes and evolution on a tectonically active margin, Deep Sea Res. Part II, 104, 93-105, 10.1016/j.dsr2.2013.06.018, 2014.
- 930 McArthur, A. D., Hartley, A. J., and Jolley, D. W.: Stratigraphic development of an Upper Jurassic deep marine syn-rift succession, Inner Moray Firth Basin, Scotland, Basin Res., 25, 285-309, https://doi.org/10.1111/j.1365-2117.2012.00557.x, 2013.
- McArthur, A. D., Crisóstomo-Figueroa, A., Wunderlich, A., Karvelas, A., and McCaffrey, W. D.: Sedimentation on structurally complex slopes: neogene to recent deep-water sedimentation patterns across the central Hikurangi subduction margin, New Zealand, Basin Res., 34, 1807-1837, https://doi.org/10.1111/bre.12686, 2022.
- 935 Métivier, F., Lajeunesse, E., and Cacas, M.-C.: Submarine canyons in the bathtub, J. Sediment. Res., 75, 6-11, https://doi.org/10.2110/jsr.2005.002, 2005.
- Micallef, A., Mountjoy, J. J., Barnes, P. M., Canals, M., and Lastras, G.: Geomorphic response of submarine canyons to tectonic activity: Insights from the Cook Strait canyon system, New Zealand, Geosphere, 10, 905-929, 10.1130/ges01040-1, 2014a.
- 940 Micallef, A., Ribó, M., Canals, M., Puig, P., Lastras, G., and Tubau, X.: Space-for-time substitution and the evolution of a submarine canyon-channel system in a passive progradational margin, Geomorphology, 221, 34-50, https://doi.org/10.1016/j.geomorph.2014.06.008, 2014b.
- Milliman, J. D. and Kao, S. J.: Hyperpycnal discharge of fluvial sediment to the ocean: Impact of super typhoon Herb (1996) on Taiwanese rivers, J. Geol., 113, 503-516, 2005.
- 945 Mitchell, N. C.: Interpreting long-profiles of canyons in the USA Atlantic continental slope, Mar. Geol., 214, 75-99, https://doi.org/10.1016/j.margeo.2004.09.005DOI:10.1016/j.margeo.2004.09.005, 2005.
- Mitchell, N. C.: Morphologies of knickpoints in submarine canyons, Geol. Soc. Am. Bull., 118, 589-605, https://doi.org/10.1130/B25772.1, 2006.
- 950 Montgomery, D. R. and Dietrich, W. E.: Source areas, drainage density, and channel initiation, Water Resour. Res., 25, 1907-1918, https://doi.org/10.1029/WR025i008p01907, 1989.
- Montgomery, D. R. and Dietrich, W. E.: Channel initiation and the problem of landscape scale, Science, 255, 826-830, https://doi.org/10.1126/science.255.5046.826DOI:10.1126/science.255.5046.826, 1992.
- 955 Mountjoy, J. J., Barnes, P. M., and Pettinga, J. R.: Morphostructure and evolution of submarine canyons across an active margin: Cook Strait sector of the Hikurangi Margin, New Zealand, Mar. Geol., 260, 45-68, 10.1016/j.margeo.2009.01.006, 2009.
- Mulder, T. and Syvitski, J. P.: Turbidity currents generated at river mouths during exceptional discharges to the world oceans, J. Geol., 285-299, 1995.Nyberg, B., Helland-Hansen, W., Gawthorpe, R. L., Sandbakken, P., Eide, C. H., Sømme, T., Hadler-Jacobsen, F., and Leiknes, S.: Revisiting morphological relationships of modern source-to-sink

格式化: 靠左

格式化: 靠左

格式化: 字型: Times New Roman

- 960 [segments as a first-order approach to scale ancient sedimentary systems, *Sediment. Geol.*, <https://doi.org/10.1016/j.sedgeo.2018.06.007>, 2018.](https://doi.org/10.1016/j.sedgeo.2018.06.007)
- Paola, C., Straub, K., Mohrig, D., and Reinhardt, L.: The “unreasonable effectiveness” of stratigraphic and geomorphic experiments, *Earth-Sci. Rev.*, 97, 1-43, <https://doi.org/10.1016/j.earscirev.2009.05.003>, 2009.
- 965 [Petit, C., Migeon, S., and Coste, M.: Numerical models of continental and submarine erosion: application to the northern Ligurian Margin \(Southern Alps, France/Italy\), *Earth Surf. Proc. Land.*, 40, 681-695, <https://doi.org/10.1002/esp.3685>, 2015.](https://doi.org/10.1002/esp.3685)
- Pettinga, L., Jobe, Z., Shumaker, L., and Howes, N.: Morphometric scaling relationships in submarine channel-lobe systems, *Geology*, 46, 819-822, <https://doi.org/10.1130/G45142.1>, 2018.
- 970 [Prélat, A., Covault, J. A., Hodgson, D. M., Fildani, A., and Flint, S. S.: Intrinsic controls on the range of volumes, morphologies, and dimensions of submarine lobes, *Sediment. Geol.*, 232, 66-76, <https://doi.org/10.1016/j.sedgeo.2010.09.010>, 2010.](https://doi.org/10.1016/j.sedgeo.2010.09.010)
- Piper, D. J. and Normark, W. R.: Processes that initiate turbidity currents and their influence on turbidites: a marine geology perspective, *J. Sediment. Res.*, 79, 347-362, 2009.
- 975 [Puig, P., Palanques, A., and Martín, J.: Contemporary sediment transport processes in submarine canyons, *Ann. Rev. Mar. Sci.*, 6, 53-77, 2014.](https://doi.org/10.1111/j.1365-3091.2010.01152.x)
- Sequeiros, O. E., Spinewine, B., Beaubouef, R. T., Sun, T. A. O., Garcia, M. H., and Parker, G.: Bedload transport and bed resistance associated with density and turbidity currents, *Sedimentology*, 57, 1463-1490, <https://doi.org/10.1111/j.1365-3091.2010.01152.x>, 2010.
- 980 [Somme, T. O., Helland-Hansen, W., Martinsen, O. J., and Thurmond, J. B.: Relationships between morphological and sedimentological parameters in source-to-sink systems: a basis for predicting semi-quantitative characteristics in subsurface systems, *Basin Res.*, 21, 361-387, <https://doi.org/10.1111/j.1365-2117.2009.00397.x>, 2009.](https://doi.org/10.1111/j.1365-2117.2009.00397.x)
- 985 [Soutter, E. L., Bell, D., Cumberpatch, Z. A., Ferguson, R. A., Spychala, Y. T., Kane, I. A., and Eggenhuisen, J. T.: The influence of confining topography orientation on experimental turbidity currents and geological implications, *Front. Earth Sci.*, 8, 1-25, <https://doi.org/10.3389/feart.2020.540633>, 2021a.](https://doi.org/10.3389/feart.2020.540633)
- [Soutter, E. L., Kane, I. A., Hodgson, D. M., and Flint, S.: The concavity of submarine canyon longitudinal profiles, *J. Geophys. Res.-Earth*, 126, e2021JF006185, <https://doi.org/10.1029/2021JF006185>, 2021b.](https://doi.org/10.1029/2021JF006185)
- 990 Spinewine, B., Sequeiros, O. E., Garcia, M. H., Beaubouef, R. T., Sun, T., Savoye, B., and Parker, G.: Experiments on wedge-shaped deep sea sedimentary deposits in minibasins and/or on channel levees emplaced by turbidity currents. Part II. Morphodynamic evolution of the wedge and of the associated bedforms, *J. Sediment. Res.*, 79, 608-628, <https://doi.org/10.2110/jsr.2009.065>, 2009.
- 995 [Strak, V., Dominguez, S., Petit, C., Meyer, B., and Loget, N.: Interaction between normal fault slip and erosion on relief evolution: Insights from experimental modelling, *Tectonophysics*, 513, 1-19, <https://doi.org/10.1016/j.tecto.2011.10.005>, 2011.](https://doi.org/10.1016/j.tecto.2011.10.005)
- [Talling, P. J., Stewart, M. D., Stark, C. P., Gupta, S., and Vincent, S. J.: Regular spacing of drainage outlets from linear fault blocks, *Basin Res.*, 9, 275-302, <https://doi.org/10.1046/j.1365-2117.1997.00048.x>, 1997.](https://doi.org/10.1046/j.1365-2117.1997.00048.x)
- [Vörösmarty, C., Fekete, B. M., Meybeck, M., and Lammers, R. B.: Geomorphometric attributes of the global system of rivers at 30-minute spatial resolution, *J. Hydrol.*, 237, 17-39, \[https://doi.org/10.1016/S0022-1694\\(00\\)00282-1\]\(https://doi.org/10.1016/S0022-1694\(00\)00282-1\), 2000.](https://doi.org/10.1016/S0022-1694(00)00282-1)
- 1000 [Wan, L., Bianchi, V., Hurter, S., Salles, T., Zhang, Z., and Yuan, X.: Morphological controls on delta-canyon-fan systems: Insights from stratigraphic forward models, *Sedimentology*, 69, 864-890, <https://doi.org/10.1111/sed.12930>, 2022.](https://doi.org/10.1111/sed.12930)

格式化: 靠左

格式化: 靠左

格式化: 字型: Times New Roman

Wan, L., Hurter, S., Bianchi, V., Salles, T., Zhang, Z., and Yuan, X.: Combining stratigraphic forward modeling and susceptibility mapping to investigate the origin and evolution of submarine canyons, *Geomorphology*, 398, 108047, <https://doi.org/10.1016/j.geomorph.2021.108047>, 2022.

格式化: 靠左

1005 Strahler, A. N.: Quantitative analysis of watershed geomorphology, *Eos, Transactions American Geophysical Union*, 38, 913-920, 1957.

Straub, K. M., Jerolmack, D. J., Mohrig, D., and Rothman, D. H.: Channel network sealing laws in submarine basins, *Geophys. Res. Lett.*, 34, 10.1029/2007gl030089, 2007.

1010 Talling, P. J., Allin, J., Armitage, D. A., Arnott, R. W. C., Cartigny, M. J. B., Clare, M. A., Felletti, F., Covault, J. A., Girardelos, S., Hansen, E., Hill, P. R., Hiseott, R. N., Hogg, A. J., Clarke, J. H., Jobe, Z. R., Malgesini, G., Mozzato, A., Naruse, H., Parkinson, S., Peel, F. J., Piper, D. J. W., Pope, E., Postma, G., Rowley, P., Sguazzini, A., Stevenson, C. J., Sumner, E. J., Sylvester, Z., Watts, C., and Xu, J. P.: Key Future Directions for Research on Turbidity Currents and Their Deposits, *J. Sediment. Res.*, 85, 153-169, 10.2110/jsr.2015.03, 2015.

1015 Tubau, X., Lastras, G., Canals, M., Micallef, A., and Ambblas, D.: Significance of the fine drainage pattern for submarine canyon evolution: The Foix Canyon System, Northwestern Mediterranean Sea, *Geomorphology*, 184, 20-37, 10.1016/j.geomorph.2012.11.007, 2013.

格式化: 字型: Times New Roman

Weill, P., Lajeunesse, E., Devauchelle, O., Metiver, F., Limare, A., Chauveau, B., and Mouaze, D.: Experimental investigation on self-channelized erosive gravity currents, *J. Sediment. Res.*, 84, 487-498, <https://doi.org/10.2110/jsr.2014.41>, 2014.

格式化: 字型: Times New Roman

格式化: 字型: Times New Roman

1020 Yu, B., Cantelli, A., Marr, J., Pirmez, C., O'Byrne, C., and Parker, G.: Experiments on self-channelized subaqueous fans emplaced by turbidity currents and dilute mudflows, *J. Sediment. Res.*, 76, 889-902, 2006.

格式化: 靠左, 缩排: 左: 0 公分, 第一行: 0 公分

格式化: 字型: Times New Roman

格式化: 靠左